Development of Organic-inorganic Hybrid Thermal Insulation Materials Based-on Polysilsesquioxane

（ポリシルセスキオキサンを利用した有機–無機ハイブリッド型断熱材料の開発）

March 2023

SAKINO TAKASE

Contents

Chapter 1 General Introduction

1.1 Energy use and CO_2 emissions

The increase in fossil fuel use over the past decades raises concerns about the future depletion of fossil resources, as well as serious environmental issues leading to the problem of climate change [2, 3]. The Paris Agreement sets a common long-term threshold for global warming below 2 ºC, preferably 1.5 ºC, in order to minimize the risks from climate change compared to pre-industrial levels [4]. The main reason for global warming is the accumulation of various greenhouse gases (GHGs) [5]. In the past few decades, the increase in worldwide fossil fuel consumption has increased GHG emissions [2, 5]. Globally, CO_2 is the most abundant anthropogenic GHG, accounting for 76% of total anthropogenic GHG emissions in 2008, and CO_2 emissions from fossil fuel use reaches 62% of total GHGs. Global emissions of CO_2 from 1850 to 2020 are summarized in Figure 1.1. Since the mid-20th century, CO_2 emissions have continued to increase rapidly and global CO_2 emissions have increased about sevenfold over the past 70 years [1, 6, 7].

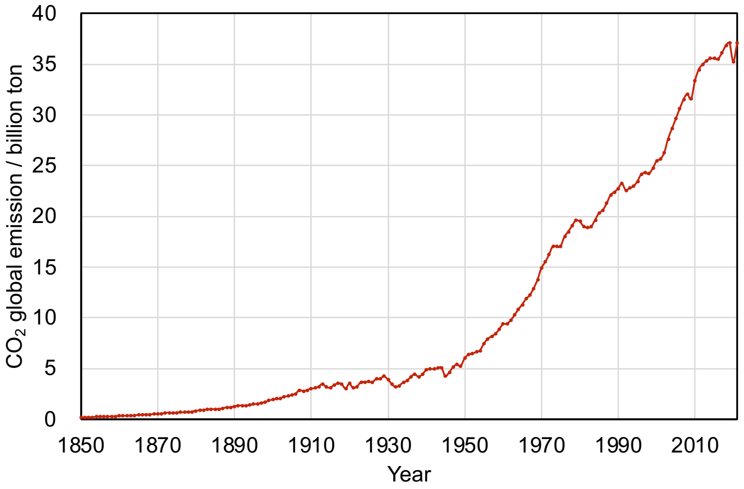

Figure 1.1 Trend in CO_2 emissions from fossil fuel combustion[1]

1.2 Thermal insulation materials

Efficient energy use in buildings is an important factor contributing to the reduction of GHG emissions. The building and construction business accounts for 30-40% of global energy consumption, mostly due to heating, ventilation, and air conditioning systems to keep people comfortable in buildings [8]. Thermal insulator is a material that slows the rate of heat flow by conduction. Other benefits of using insulators sometimes include reduced noise levels and fire protection [9]. In addition, insulators have many applications, for instance, in oil and liquefied natural gas pipelines to keep the temperature low preventing evaporation of the transported materials [8, 10]. Recent applications are in particular for automotive and aircraft engines, space technology, and heat-generating equipment in industries.

Insulation materials that have been conventionally used can be roughly classified into organic and inorganic materials. Inorganic materials including glass and rock wool account for 60% of the insulation market, while organic insulation materials such as polyurethane (PUR), polyisocyanurate (PIR), extruded polystyrene (XPS), and expanded polystyrene (EPS) account for 27% [11]. Examples of organic and inorganic insulation materials are provided below.

Organic materials

Polystyrene

Polystyrene is an organic cellular resin that is used in two types of forms, expanded polystyrene (EPS) and extruded polystyrene (XPS) [12]. EPS and XPS have a partially porous structure with excellent engineering properties, such as high energy efficiency and cost-effectiveness as a thermal insulator, soundproofing properties, and packaging versatility, and is often used for building insulation. It can be cast as a board or molded into many shapes for different purposes in the production line. EPS is made from small polystyrene beads that contain an expanding agent, e.g., pentane. These beads expand when heated with steam and are glued together at their contact points. Whereas, XPS is produced by an extrusion process of melted polystyrene resin containing a form-generating reagent or supercritical CO_2. Usually, EPS and XPS can be used only below 100 °C [13]. XPS containing flame retardants are widely used as building materials.

Polyurethane Foam

Polyurethane foam (PUR) is produced by the reaction of polyisocyanates with polyols (Figure 1.2) [14]. Primarily, isocyanates react with alcohols to produce urethane bonds in the polymer. In addition, PUR contains a variety of functional groups such as urethanes, ureas, isocyanurates, carbodiimides and uretdiones, which are formed by reactions with amines, water, ureas, urethanes, and even other isocyanates generated in the polymerization process [15-17]. Heating the PUR in an inert atmosphere, the urea and urethane decompose at 160-200 °C. PUR is also used as an expanded foam in construction, for example, as window and door seals or as a filler to fill various gaps [18]. The maximum service temperature of PUR is 120 ºC [12].

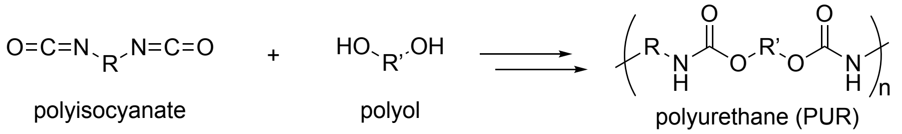

Figure 1.2 The main reaction of polyisocyanates with polyols

Polyisocyanurate Foam

Polyisocyanurate foam (PIR) is a kind of PUR foam and obtained from polyisocyanate and polyol similarly to PUR with using a higher percentage of isocyanate to form isocyanurate rings by cyclotrimerization of isocyanate (Figure 1.3). Isocyanurate is thermally stable cross-linking group and decomposes at 270-300 °C [16]. PIR is characterized by high fire resistance as well as high thermal stability. Among conventional foamed plastics, PIR has the best fire resistance. The maximum operating temperature for PIR is typically 150 ºC [14].

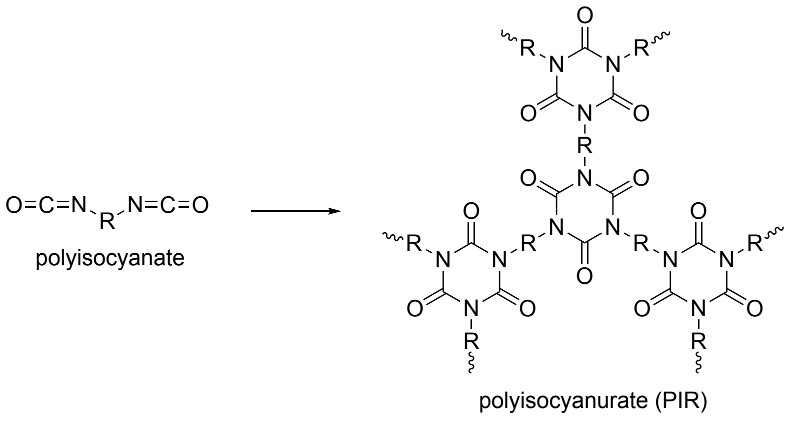

Figure 1.3 Cyclotrimerization of isocyanate

Melamine Foam

Melamine foam is produced by the reaction of melamine and formaldehyde (Figure 1.4). It exhibits a three-dimensional network skeleton with a highly porous structure. In recent years, melamine form is used as a thermal insulator for exhaust gas pipes and ducts, because of its excellent flame retardant properties due to the high nitrogen content [13, 19]. The maximum operation temperature of melamine form is approximately 200 °C, much higher than those of other polymer foams such as PUR, polystyrene, polyethylene, and polypropylene forms [13, 20, 21].

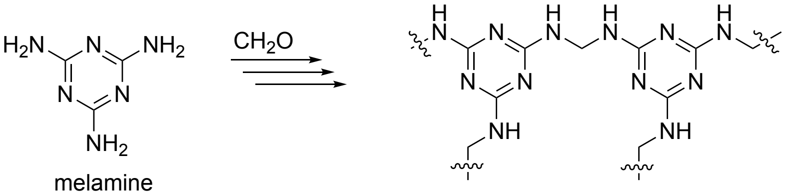

Figure 1.4 Melamine-formaldehyde resin

Cellulose Fiber

Cellulose fiber insulators are made by pulverizing paper fibers, mainly unsold newspapers and used paper [8]. It is usually treated with inorganic additives (borax: sodium borate) that inhibit flame retardants and mold growth. Cellulose is highly suitable as a filler for buildings and constructions to fill various gaps and spaces. The maximum service temperature for cellulose fiber is 80 ºC [13].

Inorganic materials

Foam glass

Most glass foams are obtained by sintering glass powder with a blowing agent [22]. Glass foam is a porous, lightweight foam material with very low thermal conductivity and desirable fire resistance. It is a sustainable insulation material that can be also manufactured from recycled waste glass. Typically, the maximum service temperature of glass foam is 500-600 °C, and potentially suitable lining material for thermal power plants [23, 24].

Rock wool and glass wool

Rock wool is typical mineral wool that is produced as boards, mats, and loose fillers. Rock wool is obtained by melting diatomaceous earth, dolerite, or other stones at temperatures around 1500 °C. The final product is manufactured by spinning at a temperature of 1400 ℃ in the form of fibers. Glass wool is produced using borosilicate glass in a similar manner. Commercial glass wool and rock wool usually contain dust-proof oil and/or phenolic resin added to improve the properties of the product and bind the fibers together, respectively. The maximum service temperature for rock wool and glass wool are approximately 800 ºC and 500ºC, respectively [12].

The above mentioned materials are used in many applications such as for building and thermal energy storage due to their low thermal conductivity. Most organic insulation materials are easy to process and provide high thermal insulation properties, but are combustible and easily melt at high temperatures, limiting their use. In contrast, inorganic insulation materials are resistant to flame and heat and can be used at high temperatures without burning or melting. However, the thermal insulation properties of inorganic insulation materials are generally lower than those of organic insulation materials. In addition, their poor processability and heavy weight make them difficult to accommodate uneven shapes and locations. From the perspective of climate change, legal obligations regarding energy consumption and related CO_2 emissions are expected to become stricter in the future. As an effective means of responding to this paradigm shift, the development of new thermal insulation materials with high heat resistance and processability is desired to explore their use in new areas of applications.

1.3 Organic-inorganic hybrid materials

Many studies have been conducted for organic-inorganic hybrid materials that have not only the properties of both organic and inorganic components, but also new functionalities arising from the synergistic effects of both components. Generally, an organic-inorganic hybrid material is defined as that with a combination of organic and inorganic components with submicron or nanoscale domain sizes, as opposed to a simple mixture and a composite material [25]. In hybrid materials, inorganic components play various roles in improving mechanical and thermal stability, modulating refractive index, or contributing to specific magnetic, electronic, redox, electrochemical, or chemical properties, while organic components provide unique functions such as stimulus responsiveness, selective binding to a guest molecule for sensing, and fine tuning of optical and electrochemical functions. For example, Qui et al. found a material that exhibits high optical transparency and high mechanical hardness by the hybrid formation of a copolymer of poly(methyl methacrylate) (PMMA) and poly(3-trimethoxysilyl propyl methacrylate) (PMSMA) with nano-sized glass particles (SiO_2) [26]. Similar hybrid films of PMMA, and SiO_2 or zirconia (ZrO_2) were prepared by Zhong and Du *et al*. Because of the formation of nano-sized organic-inorganic networks via chemical bonding, good compatibility of PMMA and inorganic particles was realized resulting in good optical transparency and thermal stability [27].

1.4 Polysilsesquioxane

Polysilsesquioxane (PSQ) is a type of organic-inorganic hybrid material consisting of a Si-O-Si inorganic siloxane network and organic substituents on silicon atoms. PSQ is represented by the general formula of $(RSiO_{1.5})_n$ where R is an organic group such as an alkyl or aryl group, typically a methyl, phenyl, or vinyl group. The organic groups (R) are selected to adjust the material properties, such as solubility, compatibility, flexibility, and surface properties according to the desired applications. The siloxane network, on the other hand, provides thermal and mechanical properties, basically improved compared to organic polymers [28, 29]. Figure 1.5 (a) shows the acid- or base-catalyzed hydrolysis/polycondensation reaction of a trialkoxysilane precursor leading to PSQ.

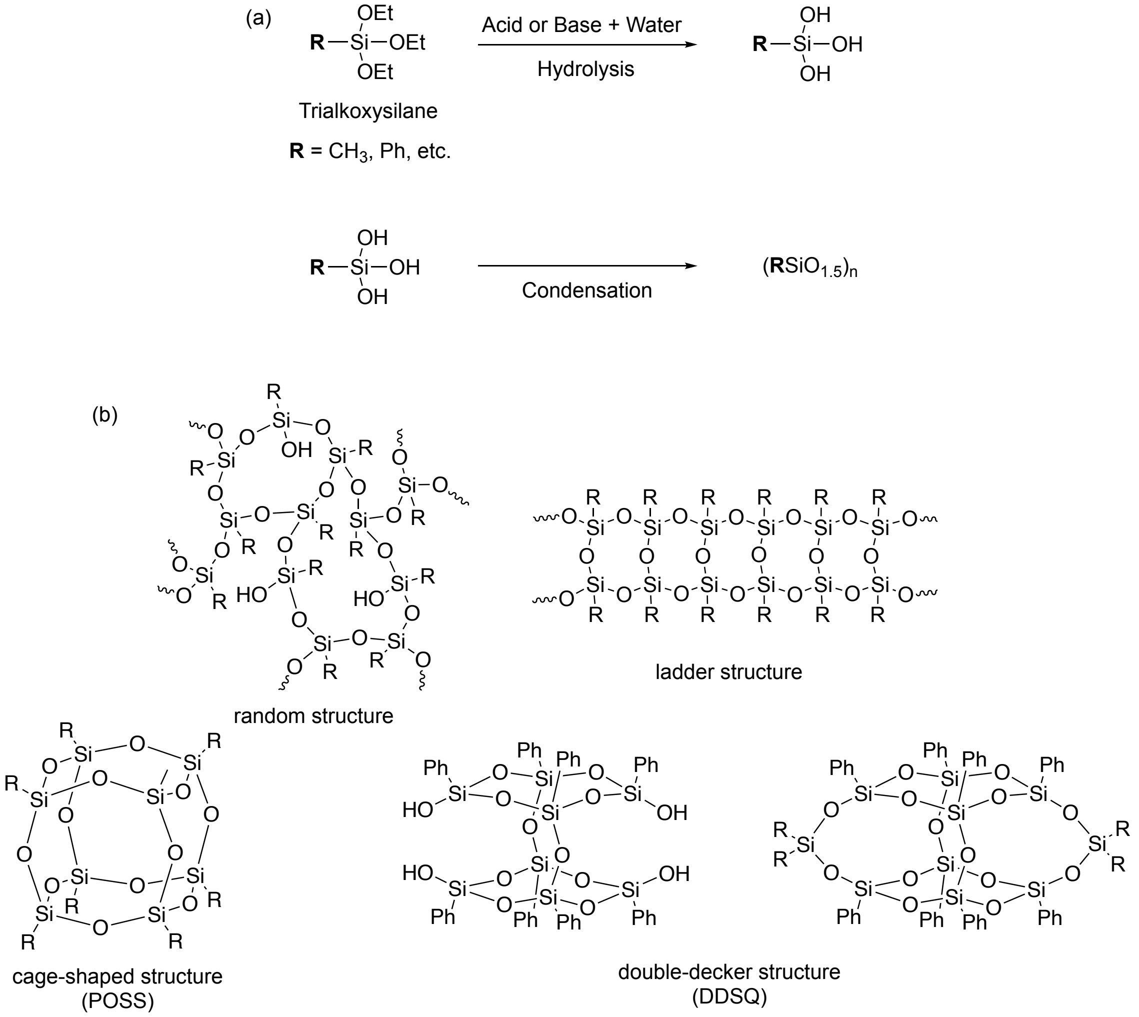

Figure 1.5 (a) Schematic diagram of the sol-gel method; (b) silsesquioxane oligomer frameworks

PSQs can be classified into categories of random, ladder, cage, and double-decker PSQs (Figure 1.5 (b)) with respect to the structural skeletal. Random PSQs are often liquid compounds when the molecular weights are low that are soluble and easy to process. In the so-called sol-gel process, random PSQ oligomer sols are calcined at high temperature after processing to form polymeric gel materials by accelerating further network formation. Random PSQs are easy to prepare and most widely studied among the PSQs [30]. Recent examples include poly(3-aminopropyl)silsesquioxane and poly(3-(2-aminoethylaminopropyl)silsesquioxane) that show excellent antifogging properties in films [31]. Applications as gas or water separation membranes [32-34], optical materials [35], low-dielectric materials [36], insulating materials [37], etc. were also investigated. Random PSQs are also studied as base materials for further hybrid formation with inorganic nano particles and as modifiers of inorganic surfaces.

Ladder PSQs are considered as one of the most regular structures among the isomers. The pseudo one-dimensional structures composed of two polysiloxane chains connected regularly without branches provides high solubility of the polymer materials. Micrometer-sized ladder-type silsesquioxanes are known to be thermally stable and processible, and high-performance self-healing and scratch resistant ladder PSQ materials have been reported [38, 39]. Phenyl and carbazole groups are known as substituents of ladder-type PSQ. Cage-shaped polyhedral oligomeric silsesquioxanes are called as POSS. In particular, POSS molecules with a highly symmetric T_8 ($R_8Si_8O_{12}$) cubic inorganic core with eight silicon atoms at the vertices have been most widely studied as the smallest and simplest silica particles with 1-3 nm in diameter, including the vertex groups [40]. Recently, double-decker silsesquioxane (DDSQ) structures have also attracted attention, featuring open or closed backbones with two or four reactive moieties; Zheng et al. reported that the inclusion of DDSQ in the main chain of polyimides improved the thermal stability and surface hydrophobicity (Figure 1.6) [25].

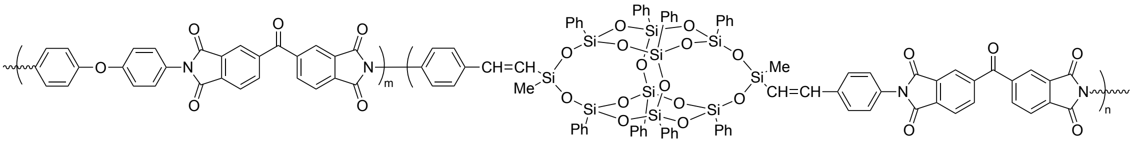

Figure 1.6 Structure of DDSQ in the main chain of polyimides

1.4.1 PSQ-based thermal insulation materials

As described above, PSQ materials are expected to have properties derived from both the organic and inorganic moieties, and therefore expected to be used as excellent thermal insulating materials with high processability, mechanical strength, thermal stability, and flame resistance.

Aerogels, defined as porous materials in which the liquid in the wet gel is replaced by gas with little or no shrinkage were first prepared by S. S. Kistler of Stanford University in the 1930s through supercritical drying methods. Since then, aerogels have been extensively investigated as functional materials such as thermal insulating materials. However, the structure fragility and the high production cost due to the use of supercritical drying have been major barriers to the development of practical applications of silica aerogels [11]. PSQ aerogels are ultra-low density nanoporous solids with excellent properties such as high surface area and porosity, low dielectric constant and thermal conductivity, and good optical transparency. In general, these PSQ aerogels are prepared using organotrialkoxysilanes as starting substrates in the two-step sol-gel method with acid or base-catalyzed reaction, followed by liquid evacuation from the wet gel by atmospheric or supercritical drying methods [41]. Rao *et al.* prepared highly flexible silica aerogels obtained using methyltrimethoxysilane (Figure 1.7) [42]. However, the capillary pressure caused cracking due to evaporation of excess water and ethanol.

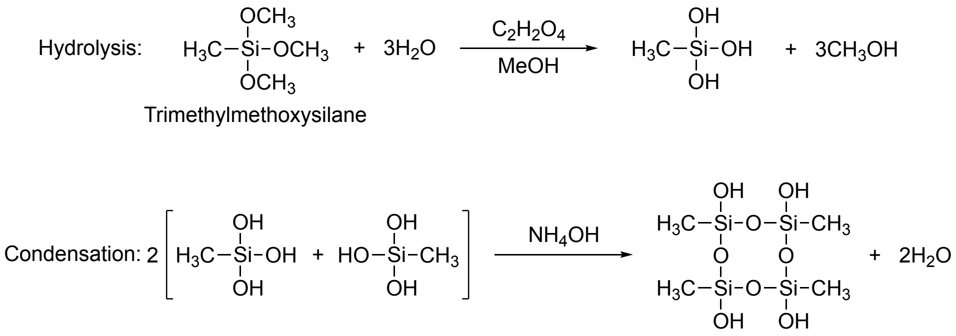

Figure 1.7 Preparation of PSQ aerogel precursor.

To obtain PSQ-based insulation materials that rigid and easy to handle, Hamada *et al.* have proposed several strategies. For example, PSQ-based thermal insulating films with an ethylene crosslinked structure were prepared by hydrosilylation of hydrosilyl- and vinylsilyl-substituted oligomethylsilisesquioxanes (MSQ-SiH and MSQ-SiVi) to exhibit high thermal stability [43]. In further efforts to improve the adiabatic performance of PSQ, POSS was embedded into the PSQ network by hydrosilylation, and it was found that the void formation around the rigid POSS structure was particularly favorable for improving the adiabatic performance (Figure 1.8) [44].

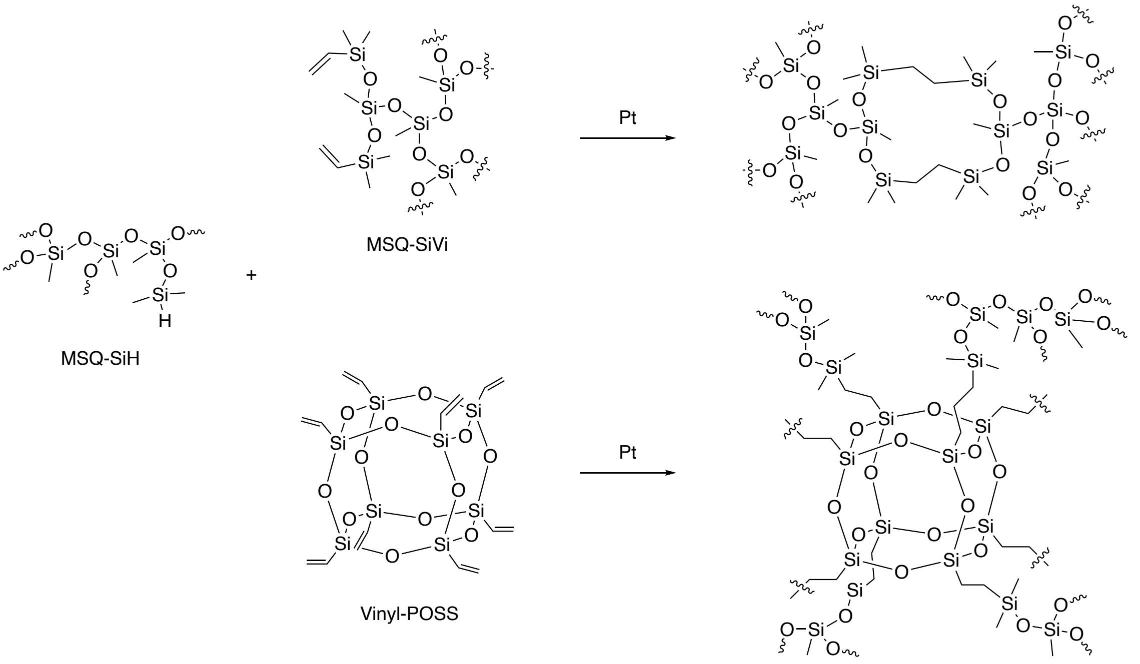

Figure 1.8 Schematic diagram of cross-linking formation by hydrosilylation between MSQ-SiH and MSQ-SiVi or Vinyl-POSS [43, 44].

1.5 Objectives and outline of this dissertation

As mentioned above, the development of high-performance thermal insulation materials is of current necessity as a solution to the problems caused by global warming and increasing energy demand. In particular, those usable in various conditions, like harsh conditions at high temperature are desired. In this dissertation, the efforts to develop PSQ-based next-generation thermal insulating materials for a wide range of applications are described. The relationship between PSQ structures and the thermal insulating properties and new approaches for the suppression of heat transfer are discussed. The contents of the chapters that follow this chapter are described below.

Chapter 2 describes the investigation of structure-thermophysical property correlation of PSQ-based gel film. PSQ with different molecular weights and residual alkoxy group contents were synthesized by changing the molar ratio of water to trialkoxysilane for the hydrolysis to investigate their effects on the adiabatic properties. To understand the effect of substituents attached to the silicon atoms of PSQs, PSQ films with different substituents attached to the silicon atoms were synthesized and the adiabatic and thermal stability of the gel films were investigated (Figure 1.9).

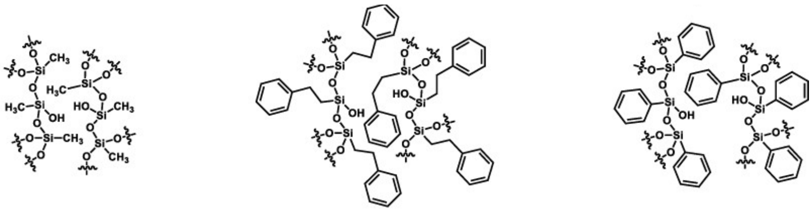

Figure 1.9 Structure of PSQ gel films for thermal insulator

In Chapter 3, alkoxy- and silanol-free oligo(methylsilsesquioxanes) (MSQ) were synthesized and hybrid films containing triallylisocyanurate (TAIC) as cross-linking units were prepared (Figure 1.10). The obtained MSQ/TAIC hybrid films were colorless, transparent, and stiff, regardless of the amount of TAIC in the PSQ network. The thermal diffusivity of the MSQ/TAIC hybrid films decreased from 1.14×10^{-7} to 1.01×10^{-7} m^2/s with an increasing amount of TAIC in the molar ratio range of 1/0.25–1/1.15 and was lower than that of a TAIC-free MSQ film prepared by the coupling reaction of MSQ-SiH (1.44×10^{-7} m^2/s) and a PSQ/tris(3-triethoxysilylpropyl)isocyanurate (TESIC) film prepared by polycondensation (1.25×10^{-7} m^2/s). A positron annihilation lifetime analysis indicated that the nature of the isocyanurate ring, rather than the formation of intramolecular void spaces, was responsible for the decrease in thermal diffusivity.

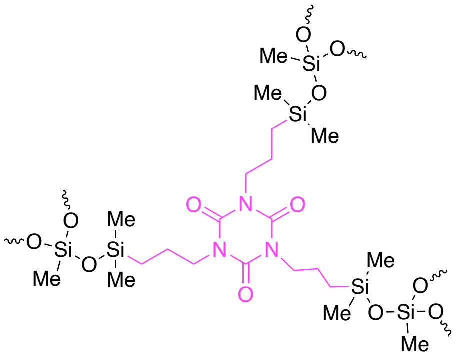

Figure 1.10 Structure of MSQ/TAIC hybrid film

In Chapter 4, the hydrosilylation reaction between hydrodimethylsilylated oligomethylsilsesquioxane and vinyl-functionalized double-decker silsesquioxane (vinyl-DDSQ), which is a highly thermally stable unit, was conducted to obtain aggregation-free DDSQ-grafted PSQ films (Figure 1.11). Unlike POSS-containing hybrid films, the high miscibility of the DDSQ molecule allowed the introduction of a high amount of vinyl-DDSQ as a crosslinker, giving colorless and transparent DDSQ-grafted PSQ films without aggregation of the DDSQ molecules. The thermal diffusivities of the DDSQ-grafted PSQ films decreased from 1.21×10^{-7} to 1.02×10^{-7} m^2/s with increasing the DDSQ amount from 5 to 25 mol%, as was similarly observed for POSS-containing hybrid films. These results indicate that the low thermal diffusivity of the DDSQ-grafted PSQ films did not stem from the formation of intramolecular void spaces but from a decrease in the crosslinking density upon the introduction of the DDSQ structure.

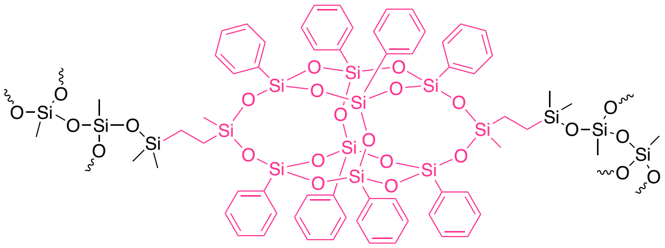

Figure 1.11 Structure of DDSQ-grafted PSQ film

In Chapter 5, the author concludes the works described in Chapters 2-4 and describes the potential of PSQ-based heat insulating materials in the future.

Chapter 2 Structure–Thermal Property Relationships of Polysilsesquioxanes for Thermal Insulation Materials

2.1 Introduction

PSQs exhibit good processability, which enables the easy preparation of their films via solution processes such as spin coating and dip coating. Hamada et al. reported a strategy for the preparation of crack- and shrinkage-free ethylene-bridged PSQ (EBPSQ) films as thermal insulation materials [43]. The introduction of SiCCSi bonds as an ethylene-bridge structure decreased the density of the PSQ film by forming intramolecular void spaces, enhancing the thermal insulation property. Furthermore, the EBPSQ films exhibited high thermal stability up to around 300 °C, which demonstrates the suitability of PSQ-based films as practical thermal insulation materials. However, the relationship between the PSQ structure and the thermal insulation property of the corresponding gel films is still not well understood. Unveiling the structure–thermal property relationship can be expected to provide a platform for the design and synthesis of thermal insulation materials.

With this aim, this chapter describes the investigation of the structure–thermal property relationship in gel films prepared from PSQs. To investigate the influence of residual alkoxy groups in PSQs on the thermal insulation property, PSQs with different molecular weights and amounts of residual alkoxy groups were synthesized by changing the molar ratio of water and trialkoxysilane for hydrolysis/condensation. To understand the influence of the substituents bonded to the silicon atom in PSQs on the thermal insulation property of their gel films, copolysilsesquioxanes (co-PSQs) with different substituents bonded to the silicon atom were synthesized by changing the monomers and the monomer ratio. Furthermore, alkoxy-free PSQs with different substituents bonded to the silicon atom were prepared via hydrolysis and polycondensation reaction of alkoxysilane under excess acid and water to investigate the influence of the substituents on the thermal insulation property and the thermal stability of the gel films.

2.2 Results and discussion

2.2.1 Synthesis of PSQ via nitrogen flow method

For the preparation of PSQs, we conducted the sol–gel reaction of triethoxymethylsilane using the nitrogen flow method according to a previously reported procedure, which allows controlling the molecular weight of PSQ and the amount of residual alkoxy groups [45]. In this method, water, catalyst, and solvent are volatilized by passing a nitrogen flow during the polycondensation, providing a mild polycondensation condition that prevents the formation of an insoluble gel. Because our purpose was to investigate the influence of residual alkoxy groups on the thermal insulation property of PSQ gel films, we synthesized polymethylsilsesquioxanes containing ethoxy groups (PSQ-Me (OEt)) with different molecular weights and amounts of residual ethoxy groups by changing the molar ratio of water and monomer, as shown in Table 2.1. As described in Experimental Section in this chapter, we used the following conditions for the synthesis: 0 °C for 10 min and room temperature for another 10 min for the hydrolysis and 90 °C for 3 h for the polycondensation reactions. In the sol–gel reaction of triethoxymethylsilane, when the molar ratio of water/monomer increased from 1.1 to 1.5, the weight-average molecular weight (M_w) of PSQ-Me (OEt) increased from 1000 to 13000 and the amount of residual ethoxy groups decreased from 22% to 7% estimated by gel permeation chromatography (GPC) and ^{1}H NMR, respectively (Table 2.1, entries 1–5). Although the obtained high-molecular-weight PSQ-Me (OEt) was highly viscous, it showed good solubility in ordinary organic solvents such as THF, acetone, and chloroform. For a water/monomer molar ratio of 1.6, a gel was formed during heating at 90 °C (Table 2.1, entry 6).

Table 2.1. Preparation of PSQ-Me (OEt) and PSQ-Me (OBu^i) via the sol–gel method[a,b]

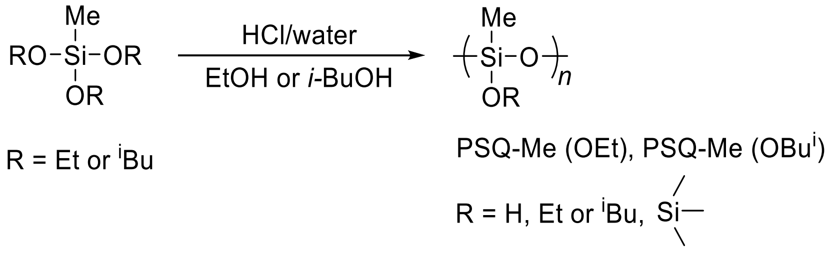

Entry	Silane	Temp. (°C)	Time (h)	Molar ratio of H_2O/silane	Residual OR (%)	M_w	M_w/M_n
1	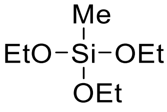 $\mathrm{MeSi(OEt)_3}$	90	3	1.1	22	1000	1.8
2		90	3	1.2	14	1800	1.9
3		90	3	1.3	10	4600	4.1
4		90	3	1.4	7	8000	3.1
5		90	3	1.5	7	13000	7.3
6		90	3	1.6	Gelation		
7	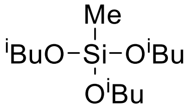 $\mathrm{MeSi(O^iBu)_3}$	100	5	1.8	19	1200	1.7
8		100	5	2.0	16	1500	1.8
9		100	5	2.5	14	1800	2.0
10		100	5	3.0	12	3000	2.7

[a] Molar ratio of monomer/HCl = 0.105.

[b] Molar ratio of solvent/monomer = 2.

In the case of the sol–gel reaction of triisobutoxymethylsilane, we conducted the polycondensation reactions at 100 °C for 5 h to completely remove the isobutyl alcohol because the boiling point of isobutyl alcohol is higher than that of ethanol. As shown in Table 2.1, the M_w of polymethylsilsesquioxane having isobutoxy groups (PSQ-Me (OBu^i)) increased from 1200 to 3000 with increasing the water/monomer molar ratio (1.8–3.0), and the amount of residual isobutoxy groups in PSQ-Me (OBu^i) also decreased from 19% to 12% (Table 2.1, entries 7–10). The hydrolysis of the isobutoxy group was slower than that of the ethoxy group because of the larger steric hindrance of the former, as was similarly described in a previous report. (18) At a small water/monomer molar ratio, PSQ-Me (OBu^i) with low molecular weight and a high amount of isobutoxy groups was obtained (Table 2.1, entry 7). Although increasing the water/monomer molar ratio up to 3 (Table 2.1, entry 10) increased the M_w to 3000 and decreased the residual isobutoxy group to 12%, these changes were not as significant as those of the sol–gel reaction of triethoxymethylsilane, particularly regarding the molecular weight.

Figure 2.1 shows the plots of M_w and residual alkoxy groups versus the water/monomer molar ratio, respectively. The M_w value of PSQ-Me (OEt) and PSQ-Me (OBu^i) increased linearly with increasing the amount of water, which indicates that the sol–gel reaction performed via the nitrogen flow method allowed controlling the molecular weight of PSQs by changing the water/monomer molar ratio. The slope of the M_w plots of PSQ-Me (OBu^i) was gentler than that of PSQ-Me (OEt). This is due to the steric hindrance of the isobutoxy group, which limits the reactivity of the residual isobutoxy group in the PSQ for the hydrolysis and the polycondensation reaction. Consequently, the sol–gel reaction of triisobutoxymethylsilane afforded a low-molecular-weight PSQ-Me (OBu^i). Nevertheless, this is no drawback to our purpose, that is, to investigate the effect of the alkoxy group on the thermal insulation property of the gel film.

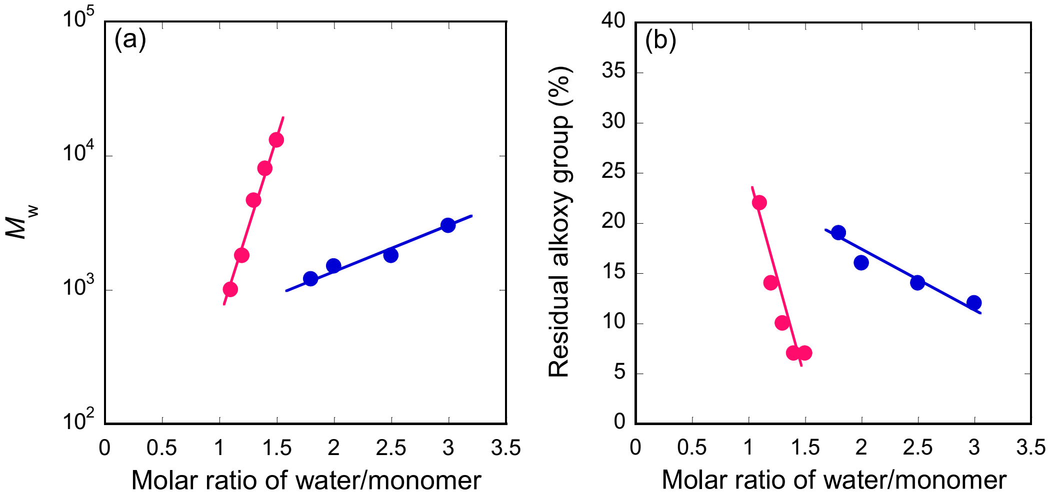

Figure 2.1 Influence of the water/monomer molar ratio on (a) the molecular weight of the polymer (Mw) and (b) the residual alkoxy group content in polymethylsilsesquioxanes prepared with triethoxymethylsilane (pink closed circles) and triisobutoxymethylsilane (blue closed circles).

Next, to investigate the influence of substituents bonded to the silicon atom on the thermal insulation property, we attempted the synthesis of PSQs using bis(triethoxysilyl)ethane and triethoxyphenylsilane via the nitrogen flow method. When we conducted the sol–gel reaction of bis(triethoxysilyl)ethane at 90 °C for 3 h with a water/monomer molar ratio of 2.2, M_w and M_w/M_n (M_n = number-average molecular weight) of the bridged PSQ were 4000 and 4.9, respectively. Unfortunately, bridged PSQ prepared from bis(triethoxysilyl)ethane contained 40% unhydrolyzed ethoxy groups. When the molar ratio of water/monomer was over 2.3, bridged PSQ formed a gel during the polycondensation reaction. Similarly, when we conducted the sol–gel reaction of triethoxyphenylsilane at 90 °C for 3 h with a water/monomer molar ratio of 2.0, M_w and M_w/M_n of the resulting polyphenylsilsesquioxane having the ethoxy group (PSQ-Ph (OEt)) were 700 and 1.4, respectively, even though the amount of residual ethoxy groups was 16%. However, PSQ-Ph (OEt) was not obtained as a soluble sol by using a water/monomer molar ratio over 2.1 due to gel formation during the polycondensation reaction, which hindered a precise comparison of the effect of substituents on the silicon atom.

To examine the influence of structure of alkoxysilane monomer on the thermal insulation property, we synthesized co-PSQ with a similar amount of residual ethoxy groups using triethoxymethysilane/bis(triethoxysilyl)ethane and triethoxymethylsilane/triethoxyphenylsilane (Table 2.2). The copolycondensation of triethoxymethylsilane and triethoxyphenylsilane (feed molar ratio = 2/1) at 90 °C for 3 h afforded PSQ-Me/Ph (2/1) (OEt) with M_w of 7900 and M_w/M_n of 1.5 (Table 2.2, entry 1). Upon increasing the feed ratio of triethoxyphenylsilane (feed molar ratio = 1/1), M_w and M_w/M_n of the corresponding co-PSQ decreased to 1900 and 1.4, respectively, most likely due to the steric hindrance of the phenyl group on the silicon atom (Table 2.2, entry 2). The amount of residual ethoxy groups in co-PSQs was similar, which is an advantage to investigate the effect of the phenyl group on the thermal insulation property. Similarly, the copolycondensations of triethoxymethylsilane and bis(triethoxysilyl)ethane at feed molar ratios of 2/1 and 1/1, respectively, at 90 °C for 3 h gave PSQ-Me/EB (2/1) (OEt) and PSQ-Me/EB (1/1) (OEt) with similar amounts of residual ethoxy groups (Table 2.2, entries 3 and 4). As in the copolymerization of triethoxymethylsilane and triethoxyphenylsilane, the molecular weight also decreased with increasing the amount of bis(triethoxysilyl)ethane because of the larger steric hindrance of the ethylene group on the silicon atom compared with that of the methyl group.

Table 2.2. Preparation of copolysilsesquioxanes (co-PSQs)[a,b]

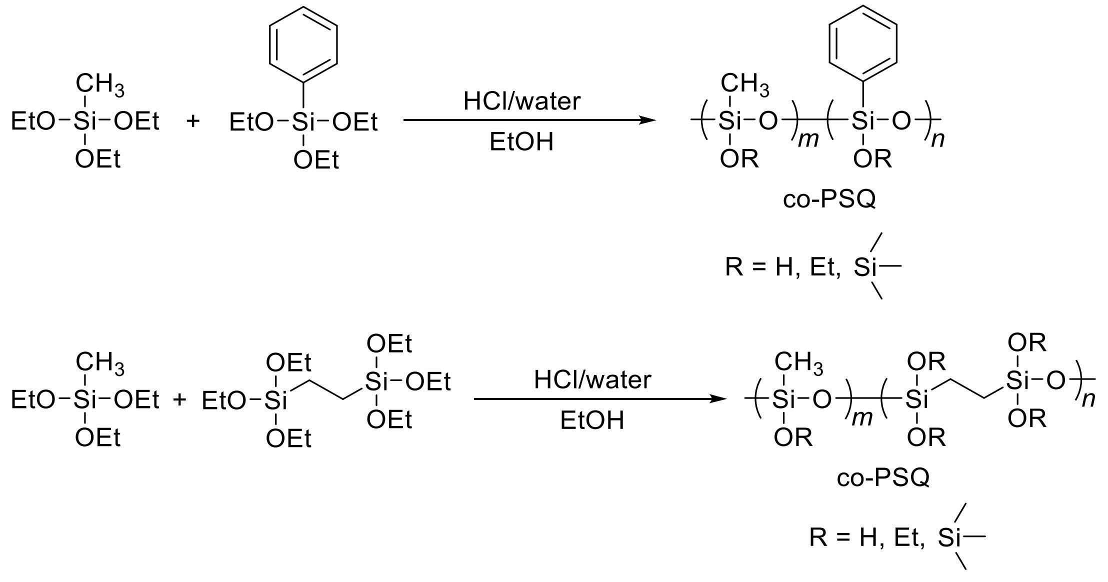

Entry	Copolysilsesquioxane	Temp. (°C)	Molar ratio of H_2O/silane	Residual OEt (%)	M_w	M_w/M_n
1	PSQ-Me/Ph (2/1) (OEt)	90	1.5	8	7900	1.5
2	PSQ-Me/Ph (1/1) (OEt)	90	1.5	10	1900	1.4
3	PSQ-Me/EB (2/1) (OEt)	90	1.5	25	4200	3.9
4	PSQ-Me/EB (1/1) (OEt)	90	1.5	30	2700	3.2

[a] Molar ratio of monomer/HCl = 0.105.

[b] Molar ratio of solvent/monomer = 2.

2.2.2 Synthesis of ethoxy-free PSQ

Having synthesized the series of PSQ-Me (OEt) and PSQ-Me (OBu^i) with different amounts of residual alkoxy groups with diverse sizes and PSQ-Me/Ph (OEt) and PSQ-Me/EB (OEt) from two kinds of monomers to investigate the influence of the residual alkoxy group and the substituents on the thermal insulation property, respectively, we considered it important to prepare an ethoxy-free PSQ to investigate the influence of the substituents on the silicon atom in more detail. In a previous paper, we reported the synthesis of oligomethylsilsesquioxane and the subsequent capping reaction with chlorodimethylsilane. Intermediate oligomethylsilsesquioxane, which was synthesized at 0 °C by using excess water and HCl, had almost no ethoxy groups [43]. On the basis of this result, we attempted the synthesis of ethoxy-free PSQ from bis(triethoxysilyl)ethane following the same procedure. However, the product was not isolated upon extraction after hydrolysis of bis(triethoxysilyl)ethane. Meanwhile, ethoxy-free PSQ-Ph was easily synthesized under reflux for 3 h by using excess water and HCl, but the content of residual ethoxy groups was only 2%, which was sufficient to investigate the influence of the substituents on the thermal insulation property. Similarly, the residual ethoxy group content in ethoxy-free polyphenethylsilsesquixane (PSQ-Phe) synthesized from triethoxyphenethylsilane was also negligible (4%). As shown in Table 2.3, the molecular weight of PSQ-Ph and PSQ-Phe synthesized under reflux condition was considerably low because ethanol as the reaction solvent was not volatilized during the polycondensation reaction, which contrasts with the result of the sol–gel reaction conducted via the nitrogen flow method [45]. Nevertheless, their molecular weight was sufficient to investigate the influence of the substituted group on the silicon atom.

Table 2.3. Preparation of PSQ-Me, PSQ-Ph, and PSQ-Phe via the sol–gel method[a,b]

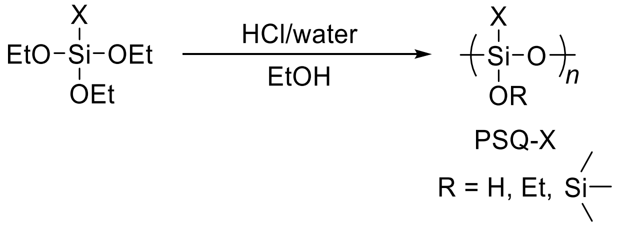

Entry	X	Solvent	Temp. (°C)	Molar ratio of H_2O/silane	Residual OEt (%)	M_w	M_w/M_n
1[c]	CH_3–	THF	0	15	2	450	1.3
2	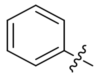	ethanol	reflux	15	2	700	1.3
3	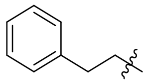	ethanol	reflux	15	4	1800	1.6

[a] Molar ratio of monomer/HCl = 6.67.

[b] Molar ratio of solvent/monomer = 5.

[c] These data were obtained from Reference [43].

2.2.3 Preparation of freestanding gel films

The conditions for the preparation of freestanding gel films are summarized in Table 2.4. We successfully prepared freestanding gel films of PSQ-Me (OEt) in a poly(tetrafluoroethylene-*co*-perfluoroalkylvinyl ether) (PFA) vial with an inner diameter of 18.4 mm. First, we placed a 20 wt% THF solution of PSQ-Me (OEt) in the vial and heated the polymer solution at 80 °C for 1 h to remove the solvent and then at 160 °C for 1 h to slowly start the cross-linking reaction. Finally, we heated the obtained product at 200 °C for 2 h to complete the cross-linking reaction and took the final product from the PFA vial. The freestanding gel film prepared from PSQ-Me (OEt) was transparent and stiff after heating at 200 °C for 2 h, whereas PSQ-Me (OBu^i) required 4 h at 200 °C to complete the cross-linking reaction and produce a transparent and stiff freestanding gel film. Therefore, we fixed the temperature for the cross-linking reaction at 200 °C and changed the heating time for the preparation of each freestanding film. Similarly, PSQ-Ph and PSQ-Phe required 3–6 h at 200 °C to produce freestanding gel films because of the steric hindrance of the substituents on the silicon atom. A freestanding gel film of PSQ-Ph was not obtained due to dewetting of PSQ-Ph on the PFA vial during heating of the polymer solution. Therefore, the PSQ-Ph film was prepared onto a Kapton film by using an applicator. In contrast, PSQ-Me/EB (OEt) easily formed gel films within 1 h at 200 °C because of the high degree of cross-linking sites in the ethylene-bridged structure. As shown in Table 2.4, partial cracks were only observed in the gel film of PSQ-Me/EB (OEt) probably due to its high cross-linking ratio affording a too stiff film that shrunk upon elimination of unhydrolyzed ethoxy groups. In fact, a gel film of ethylene-bridged polysilsesquioxane prepared from bis(triethoxysilyl)ethane was reported to contain many cracks upon heating at 200 °C for 20 min [43].

Table 2.4. Results and conditions for the preparation of freestanding gel films

	Temperature (°C)	Time (h)	Film preparation method	Film state
PSQ-Me (OEt)	200	2	drop casting	transparent
PSQ-Me (OBu^i)	200	4	drop casting	transparent
PSQ-Me/Ph (OEt)	200	4	drop casting	transparent
PSQ-Me/EB (OEt)	200	1	drop casting	partially crack
PSQ-Ph	200	3	applicator coating	transparent
PSQ-Phe	200	6	drop casting	transparent

2.2.4 Thermal diffusivity of the PSQ films

To investigate the influence of the residual alkoxy group in PSQ on the thermal insulation property, we measured the thermal diffusivities of the freestanding gel films with thickness of 300–700 μm prepared from PSQ-Me (OEt) and PSQ-Me (OBu^i) and plotted them as a function of the residual alkoxy group content (Figure 2.2 and Table 2.5). In this experiment, we assumed that the trend in the amount of residual alkoxy group was not changed between polymer and gel film. Unfortunately, the low amount of residual ethoxy groups in the gel film hindered its quantitative determination by Fourier transform infrared (FT-IR) spectroscopy.

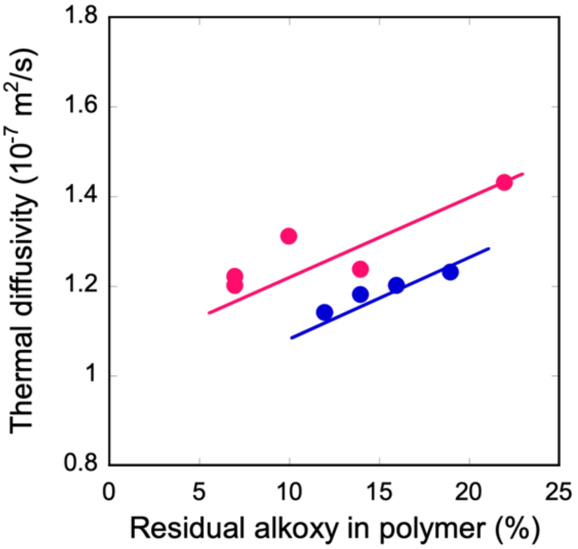

Figure 2.2 Influence of the residual alkoxy group content in the polymer on the thermal diffusivity of gel films prepared from polymethylsilsesquioxanes containing ethoxy groups (pink closed circles) and triisobutoxy groups (blue closed circles).

Table 2.5. Thermal diffusivities of the gel films

Entry	Polysilsesquioxane	M_w	M_w/M_n	Residual OEt (%)	Thermal diffusivity (m^2/s)
1	PSQ-Me (OEt)	1000	1.8	22	1.43×10^{-7}
2	PSQ-Me (OEt)	1800	1.9	14	1.24×10^{-7}
3	PSQ-Me (OEt)	4600	4.1	10	1.31×10^{-7}
4	PSQ-Me (OEt)	8000	3.1	7	1.20×10^{-7}
5	PSQ-Me (OEt)	13000	7.3	7	1.22×10^{-7}
6	PSQ-Me (OBu^i)	1200	1.7	19	1.23×10^{-7}
7	PSQ-Me (OBu^i)	1500	1.8	16	1.20×10^{-7}
8	PSQ-Me (OBu^i)	1800	2.0	14	1.18×10^{-7}
9	PSQ-Me (OBu^i)	3000	2.7	12	1.14×10^{-7}
10	PSQ-Me/Ph (2/1) (OEt)	7900	1.5	8	1.17×10^{-7}
11	PSQ-Me/Ph (1/1) (OEt)	1900	1.4	10	1.07×10^{-7}
12	PSQ-Me/EB (2/1) (OEt)	4200	3.9	25	1.42×10^{-7}
13	PSQ-Me/EB (1/1) (OEt)	2700	3.2	30	1.47×10^{-7}
14	PSQ-Me[a]	450	1.3	2	1.36×10^{-7}
15	PSQ-Ph	700	1.3	2	0.94×10^{-7}
16	PSQ-Phe	1800	1.6	4	1.17×10^{-7}

[a]These data were obtained from Reference [43].

The thermal diffusivities of the freestanding gel films prepared from PSQ-Me (OEt) decreased from 1.43 × 10^{-7} to 1.20 × 10^{-7} m^2/s with decreasing the residual ethoxy group content from 22% to 7%. Similarly, the thermal diffusivities of the freestanding gel films prepared from PSQ-Me (OBu^i) decreased from 1.23 × 10^{-7} to 1.14 × 10^{-7} m^2/s with decreasing the residual isobutoxy group content from 19% to 12%, although this sample showed lower thermal diffusivities in the whole range of the residual isobutoxy group content compared with the PSQ-Me (OEt)-derived gel films. Interestingly, a clear influence of the alkoxy group on the thermal insulation property was observed: the presence of isobutoxy groups in PSQ enhanced the thermal insulation property compared with the residual ethoxy group, whereas the increase in the residual ethoxy group content decreased the thermal insulation property. The thermal diffusivity of gel films might be also relevant with the molecular weight of PSQ-Me (OEt) and PSQ-Me (OBu^i). The PSQ with the high molecular weight forms a high-level network structure, and the heat conduction occurs via the siloxane network. However, the thermal diffusivity of PSQ-Me (OEt)- and PSQ-Me (OBu^i)-derived gel films unexpectedly decreased with increasing the molecular weight. In addition, PSQ-Me (OBu^i) forms gel films with low thermal diffusivity even though the molecular weight of PSQ-Me (OBu^i) was lower than PSQ-Me (OEt). On the freestanding film preparation, treatment of PSQs at high temperature enhanced the polymer network by the cross-linking and intermolecular condensation with respect to residual silanol units to yield insoluble gels, regardless of the molecular weight of pristine polymer. Therefore, it is concluded that the thermal diffusivity of gel film was affected primarily by the alkoxy group in PSQ.

Considering the bulkiness of the isobutoxy group, we attributed the decrease in the thermal diffusivity of the freestanding gel film prepared from PSQ-Me (OBu^i) to the residual isobutoxy groups forming large intramolecular void spaces. This hypothesis was supported by the results of a positron annihilation lifetime analysis. We measured the lifetime spectra of PSQ-Me (OEt) and PSQ-Me (OBu^i) having similar amounts of alkoxy groups (Table 2.5, entries 2 and 8), separated them into four components, and determined the longest lifetime corresponding to the pick-off annihilation of ortho-positronium. Using a numerical Laplace inversion technique, we obtained the probability density function of the annihilation rate. As shown in Figure 2.3, the peak position of PSQ-Me (OBu^i) was shifted to a longer time region compared with that of PSQ-Me (OEt). The

τ_3 value of PSQ-Me (OBu^i) (4.81 ± 0.01 ns) was larger than that of PSQ-Me (OEt) (3.74 ± 0.01 ns), which indicates that the free-volume spaces of PSQ-Me (OBu^i) were larger than those in the PSQ-Me (OEt) film. We estimated the radius of free-volume holes (*R*) for PSQ-Me (OEt) and PSQ-Me (OBu^i) to be 0.41 and 0.47 nm, respectively, using the Tao–Eldrup equation [46, 47]. The calculated hole volume of PSQ-Me (OBu^i) was 0.42 nm^3, which was apparently larger than that of PSQ-Me (OEt) (0.29 nm^3). This explains the lower thermal diffusivities of the gel films prepared from PSQ-Me (OBu^i) in the whole range of residual alkoxy group content compared with that of the PSQ-Me (OEt) gel films. Considering the formation of intramolecular void spaces in the freestanding gel films as a result of the presence of the residual alkoxy groups, the thermal diffusivity could be expected to decrease with increasing the amount of residual alkoxy groups. However, the thermal diffusivity of the freestanding gel films increased with increasing the residual alkoxy group content (Figure 2.2). This increase in the thermal diffusivity might be due to the polar alkoxy group enhancing the thermal conductivity of the film.

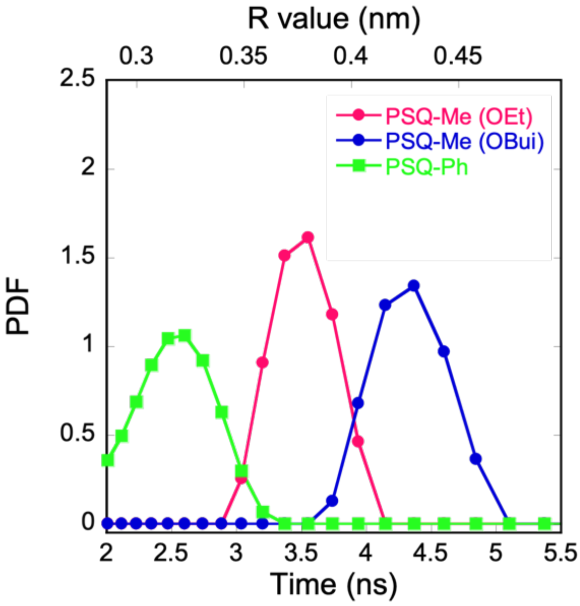

Figure 2.3 Probability density function (PDF) of the lifetimes of ortho-positronium in PSQ-Me (OEt) and PSQ-ME (OBu^i) and PSQ-Ph.

Next, to investigate the influence of substituents bonded to the silicon atom on the thermal insulation property, we measured the thermal diffusivities of freestanding gel films prepared from co-PSQs, and the results are shown in Table 2.5. The thermal diffusivities of the gel films of PSQ-Me/Ph (2/1) (OEt) and PSQ-Me/Ph (1/1) (OEt) were 1.17×10^{-7} and 1.07×10^{-7} m^2/s, respectively, which showed a dependence on the phenyl group content and were clearly lower than that of PSQ-Me (OEt) having a similar amount of ethoxy groups (1.31×10^{-7} m^2/s) (Table 2.5, entries 3, 10, and 11). Considering that the amount of ethoxy group was similar (Table 2.5, entries 10 and 11), we attributed the improvement of the thermal insulation property to the bulky phenyl group on the silicon atom creating intramolecular voids spaces. In contrast, the gel films of PSQ-Me/EB (2/1) (OEt) and PSQ-Me/EB (1/1) (OEt) showed thermal diffusivities of 1.42×10^{-7} and 1.47×10^{-7} m^2/s (Table 2.5, entries 12 and 13), respectively, which were similar to that of PSQ-Me (OEt) with an ethoxy group content of 22%. The ethylene-bridged structure in PSQ increased the thermal diffusivity of its gel film. However, we reported in a previous paper that the ethylene-bridged structure decreased the thermal diffusivity of an EBPSQ film due to the formation of intramolecular void spaces [43]. For example, an EBPSQ film prepared via hydrosilylation reaction exhibited a low thermal diffusivity of 1.15×10^{-7} m^2/s and a density of 1.13 g/cm^3, which was inconsistent with the high thermal diffusivities in the gel films of PSQ-Me/EB (2/1) (OEt) and PSQ-Me/EB (1/1) (OEt) [43]. This difference could be due to the presence of unhydrolyzed ethoxy groups in the EBPSQ synthesized from bis(triethoxysilyl)ethane via the nitrogen flow method, which increased the thermal diffusivity as mentioned above.

Unfortunately, the influence of the ethoxy group on the heat conduction in the PSQ films was not clear. Recently, Naka *et al* reported beads-on-string-shaped polyurea with high thermal conductivity as a result of the formation of an extended hydrogen-bond network promoted by the hydrophobic cage-type silsesquioxane in the main chain of polyurea [48].Accordingly, in the present PSQ films, the polar ethoxy groups could form hydrogen bonds with silanol, leading to a refinement film with enhanced thermal diffusivity.

We also measured the thermal diffusivities of the gel films prepared from ethoxy-free PSQ to gain a deeper understanding on the influence of substituents bonded to the silicon atom (Table 2.5, entries 14–16). As reported in a previous paper, despite not containing the polar ethoxy group, a PSQ-Me film prepared from oligomethylsilsesquioxane exhibited a high thermal diffusivity of 1.36×10^{-7} m^2/s because oligomethylsilsesquioxane formed a highly cross-linked structure [43]. Meanwhile, the gel film prepared from PSQ-Ph exhibited a low thermal diffusivity of 0.94×10^{-7} m^2/s. As discussed for the thermal diffusivity of the PSQ films, we expected that the phenyl group on the silicon atom decreased the thermal diffusivity of the PSQ film due to the formation of intramolecular void spaces. However, the lifetime spectrum of PSQ-Ph contradicted this hypothesis, as shown in Figure 2.3. The obtained $\tau_3$value was 2.96 ± 0.01 ns, which corresponds to the lowest lifetime among the films evaluated. For PSQ-Ph, the Tao–Eldrup equation afforded an *R* value of 0.36 nm, and the hole volume was 0.20 nm^3. Therefore, the thermal diffusivity of the PSQ films containing an aromatic group might decrease due not only to the formation of intramolecular void spaces but also to the influence of the substituent bonded to the silicon atom on the cross-linking density; namely, PSQ-Ph might form a low density network structure, even though the effect of the phenyl group on the silicon atom is still unclear.

Similarly, the PSQ-Phe film showed a low thermal diffusivity of 1.17×10^{-7} m^2/s because of the presence of the bulky phenyl group (Table 2.5, entry 16). We expected that the ethylene-bridged structure between the phenyl group and the silicon atom would create intramolecular void spaces, further decreasing the thermal diffusivity. However, the thermal diffusivity of the PSQ-Phe film was higher than that of the PSQ-Ph film. This might be due to the low steric hindrance of the phenethyl group around the silicon atom.

Overall, although the heat conduction in PSQ materials is complicated and the detailed mechanism is not clear, the residual alkoxy groups and the substituents on the silicon atom significantly influenced the thermal insulation property of the gel films.

2.2.5 Thermal stability of the PSQ films

As mentioned in Introduction of this thesis (Chapter 1), the thermal stability of thermal insulation materials is also important for their application under severe conditions such as high temperature. To study the influence of the substituents bonded to the silicon atom on the thermal stability of the gel films, we performed a TGA analysis in air on the ethoxy-free PSQ-derived gel films because ethoxy groups are usually unstable and decompose easily at lower temperature than other organic groups. As previously reported, a gel film prepared from PSQ-Me showed high thermal stability and was stable up to 400 °C (Figure 2.4) [43]. In this study, the PSQ-Me film showed a 5% weight loss temperature (T_d^5) of 436 °C and a 10% weight loss temperature (T_d^{10}) of 481 °C (Table 2.6). In this temperature region, some products such as methane, hydrogen, carbon monoxide, and carbon dioxide might be generated by thermal decomposition [49].

Table 2.6. Thermal properties of gel films prepared from PSQ-Me, PSQ-Ph, and PSQ-Phe[a]

	Residual OEt (%)	T_d^5 (°C)	T_d^{10} (°C)
PSQ-Me[b]	2	436	480
PSQ-Ph	2	485	560
PSQ-Phe	4	280	327

[a] Measured at a heating rate of 10 °C/min under an air flow of 100 mL/min.

[b] These data were obtained from Reference [43].

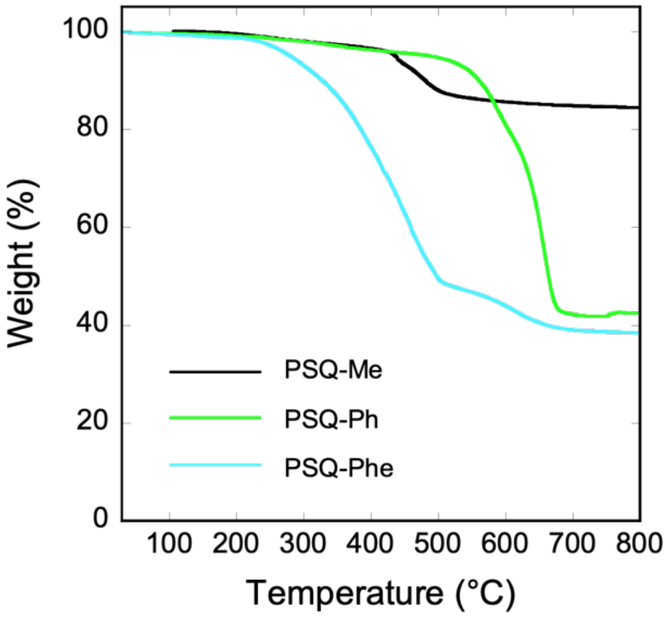

Figure 2.4 Thermogravimetric analysis traces of gel films prepared from PSQ-Me, PSQ-Ph, PSQ-Phe measured at a heating rate of 10 °C/min under an air flow of 100 mL/min. The data for PSQ-Me were obtained from ref [43].

Polyphenylsilsesquioxane typically has high thermal stability, and the main degradation mechanism is the formation of a phenyl radical [49]. Indeed, the thermal stability of the PSQ-Ph film was considerably higher, with T_d^5 and T_d^{10} values of 485 and 560 °C, respectively. A similar enhancement of the thermal property of a polymer by the phenyl group was observed for a phenyl-modified MQ resin, which was more resistant to thermal oxidation than a related methyl MQ resin [50]. According to the literature, this phenomenon was attributed to the strengthening of the siloxane bond by an increased participation of the lone pair electrons on the oxygen atom [50]. Very recently, Kickelbick's group also reported that polyphenylsilsesquioxane gel prepared from phenyltrimethoxysilane show high T_d^5 and T_d^{10}over 500 °C [51]. However, the thermal stability of the PSQ-Phe film was lower than that of the gel films of PSQ-Me and PSQ-Ph even though PSQ-Phe also contained a phenyl ring. Thus, the T_d^5 and T_d^{10} of the PSQ-Phe film decreased to 280 and 327 °C, respectively. According to the literature, poly(benzyl acrylate) is thermally more unstable than poly(methyl acrylate) and decomposes at 270 °C into carbon dioxide, benzyl alcohol, and low-molecular-weight polymer [52]. This is due to the nature of the benzyl group, in which the carbon at the benzyl position oxidizes around 250 °C. The glass transition temperatures (T_g) of PSQ-Me, PSQ-Ph, and PSQ-Phe were investigated by DSC. However, the gel films exhibited no distinct T_g over the temperature range from −60 to 120 °C. Organoalkoxysilanes are known to form melting gels through hydrolysis and polycondensation reactions under certain conditions [51, 53, 54]. In previous studies, the T_g of a melting gel prepared from phenyl-substituted trialkoxysilane was below 100 °C [51, 53, 54]. However, PSQ-Ph showed no distinct T_g because it was prepared at 200 °C to form the cross-linked network. Indeed, a glass-like material prepared from phenyltrimethoxysilane at 200 °C exhibited no T_g because the formation of a glass-like material from a melting gel above 200 °C is an irreversible consolidation process [51].This indicates that PSQ-Ph formed a well-grown cross-linked network and was thermally stable. Therefore, it is a more suitable thermal insulation material than organic materials. It can be concluded that the substituents bonded to the silicon atom have a significant influence on the thermal stability of the films. Particularly, the phenyl group as a substituent confers the polymer films with stability, rendering them suitable as heat-resistant materials.

2.3 Conclusions

In this study, we prepared a series of PSQs via the sol–gel reaction to investigate the influence of residual alkoxy groups and substituents on the thermal insulator property of the corresponding freestanding gel films.

The thermal diffusivities of freestanding gel films prepared from PSQ-Me (OEt) and PSQ-Me (OBu^i) decreased with decreasing the amount of residual alkoxy groups. Furthermore, the thermal diffusivity of the PSQ-Me (OBu^i) freestanding gel film was lower than that of freestanding PSQ-Me (OEt) gel films. Interestingly, a clear influence of the alkoxy group on the thermal insulator property was observed; that is, the presence of the isobutoxy group in the polymer enhanced the thermal insulation property, whereas increasing the residual alkoxy group content decreased the thermal insulation property.

The substituents on the silicon atom also affected the thermal insulator property. The gel films prepared from PSQ-Me/Ph (2/1) (OEt) and PSQ-Me/Ph (1/1) (OEt) exhibited thermal diffusivities of 1.17×10^{-7} and 1.07×10^{-7} m^2/s, respectively, which were clearly lower than that of the PSQ-Me (OEt) gel film having a similar residual ethoxy group content ($1.31 \times 10^{-7} m^2/s$). The bulky phenyl group on the silicon atom apparently decreased the thermal diffusivity depending on the amount of phenyl group (PSQ-Me/Ph (1/1) (OEt) < PSQ-Me/Ph (2/1) (OEt) < PSQ-Me (OEt)). To precisely understand the influence of substituents, we synthesized ethoxy-free PSQs such as PSQ-Me, PSQ-Ph, and PSQ-Phe and measured the thermal diffusivities of their gel films. The gel films prepared from PSQ-Ph and PSQ-Phe showed low thermal diffusivities of 0.94×10^{-7} and 1.17×10^{-7} m^2/s, respectively, compared with that of the PSQ-Me gel film (1.36×10^{-7} m^2/s). This indicates that the phenyl and phenethyl groups on the silicon atom clearly decreased the thermal diffusivity of the films by the formation of intramolecular void spaces and the change in the cross-linking density.

The thermal stability of the PSQ-Ph film was considerably higher than that of the PSQ-Me and PSQ-Phe films, and its T_d^5 and T_d^{10} values were 485 and 560 °C, respectively. However, despite the presence of a phenyl ring in PSQ-Phe, its thermal stability was lower than that of PSQ-Me and PSQ-Ph, exhibiting T_d^5 and T_d^{10} values of 280 and 327 °C, respectively. We attribute this result to the inherent instability of the benzyl group at high temperature in air. Overall, this study demonstrates that the thermal stability of gel films prepared from PSQ was considerably affected by the substituents on the silicon atom.

2.4 Experimental

Materials

Triethoxymethylsilane, triethoxyphenylsilane, and trichloromethylsilane were purchased from Tokyo Chemical Industry Co., Ltd. (Tokyo, Japan). Trichlorophenethylsilane was purchased from Shinetsu Chemical Co., Ltd. (Tokyo, Japan). Bis(triethoxysilyl)ethane was purchased from Oakwood Products, Inc. Ethanol (super dehydrated) was purchased from FUJIFILM Wako Pure Chemical Co., Ltd. (Osaka, Japan). All these chemicals were used as received. Tetrahydrofuran (THF), toluene, 2-methyl-1-propanol, triethylamine, and 6 mol/L hydrochloric acid (HCl) were purchased from FUJIFILM Wako Pure Chemical Co., Ltd. (Osaka, Japan). THF, toluene, and 2-methyl-1-propanol were distilled over calcium hydride before use. Triethylamine was distilled and dried over potassium hydroxide, and 6 mol/L HCl was used as received without purification. Water was purified by using a Millipore Mill-Q UV system and had a resistance of 18.2 MΩ cm and a total organic carbon content of <10 ppb.

Characterization

^{1}H nuclear magnetic resonance (NMR) measurements were performed on a Varian 400 MHz spectrometer in deuterium chloroform ($CDCl_3$) by using residual chloroform as an internal standard (7.26 ppm) for chemical shift referencing. ^{13}C NMR measurements were performed on a Varian 400 MHz spectrometer and a Varian 500 MHz spectrometer. ^{29}Si NMR spectra were measured by using a Varian 500 MHz spectrometer, and tetramethylsilane was used as an internal standard. GPC was performed on a Shimadzu LC-20AD system equipped with a RID-10A detector and three directly connected TSKgel G6000H/G4000H/G2000H columns. THF was used as an eluent at 40 °C and a flow rate of 1 mL/min, and polystyrene standards were used for calibration. Thermogravimetric analysis (TGA) data were obtained with a SII EXSTAR TG-DTA6200 thermal analyzer at a heating rate of 10 °C/min under an air flow of 100 mL/min. Differential scanning calorimetry (DSC) measurements were performed on an SII EXSTAR

DSC6200 under a nitrogen flow of 100 mL/min. Heating and cooling were performed at 10 °C/min over the temperature range −60 to 120 °C. Thermal diffusivity measurements of the films were performed on an ai-phase Mobile M3 type 1 system. A plate of zirconium oxide with a thickness of 500 μm was used for calibration. The measurements were repeated nine times, and the averaged thermal diffusivity was calculated. Positron lifetime measurements were performed by using a system based on a digital oscilloscope. Positron lifetime measurements were performed using a ^{22}Na source (400 kBq). The lifetime spectrum S_{LT} (t) is expressed by the following equation (2.1)

$$S_{LT}(\mathrm{t}) = \sum \lambda_i \, I_i \exp(-\lambda_i t) \tag{2.1}$$

where λ_i and I_i are the annihilation rate and the relative intensity of the positron of the *i*th component, respectively ($\sum I_i = 1$). The lifetime of positron λ_i is given by $1/\lambda_i$. The observed spectra were analyzed with a time resolution of 185 ps (full width at half-maximum) using the RESOLUTION computer program. The radius of free-volume holes, R (nm), was calculated according to the following Tao–Eldrup equation (2.2) [46, 47]

$$\frac{1}{\tau_3} = 2 \times \left[1 - \frac{R}{R_0} + \frac{1}{2\pi}\sin\left(\frac{2\pi R}{R_0}\right)\right] \tag{2.2}$$

where R_0 is a fitted empirical electron-layer thickness ($=R + 0.1656$ nm). The hole volume V(nm^3) was calculated according to the following equation (2.3)

$$V = \frac{4}{3}\pi R^3 \tag{2.3}$$

Synthesis of triethoxyphenethylsilane

In a 200 mL flask, triethylamine (25.6 g, 252 mmol), ethanol (12.3 g, 268 mmol), and 105 mL of toluene were added and cooled in an ice/water bath. Trichlorophenethylsilane (17.2 g, 72.0 mmol) was slowly added dropwise at 0 °C under an argon atmosphere, and the reaction mixture was then refluxed for 3 h. The resulting triethylamine salt was removed by filtration, and the solution was evaporated under reduced pressure. The residue was distilled under reduced pressure (114.0–118.5 °C/6 mmHg) to give triethoxyphenethylsilane (11.1 g, 58%) as a colorless liquid. ^{1}H NMR (400 MHz, $CDCl_3$, ppm): $\delta = 7.19$ (5H, m), 3.83 (6H, q, $J = 7$ Hz), 2.78 (2H, m), 1.25 (9H, t, $J = 7$ Hz), 1.02 (2H, m). ^{13}C NMR (125 MHz, $CDCl_3$, ppm): $\delta = 144.9$, 128.2, 125.0, 57.5, 28.0, 17.5, 12.5. ^{29}Si NMR (100 MHz, $CDCl_3$, ppm): $\delta = -45.8$.

Synthesis of triisobutoxymethylsilane

In a 200 mL flask, triethylamine (14.6 g, 144 mmol), isobutyl alcohol (11.3 g, 153 mmol), and 60 mL of toluene were added and cooled in an ice/water bath. Trichloromethylsilane (6.1 g, 41 mmol) was slowly added dropwise at 0 °C under an argon atmosphere. After refluxing for 3 h, the reaction mixture was filtrated to remove the resulting triethylamine salt, and the solution was evaporated under reduced pressure. The residue was distilled under reduced pressure (80–83 °C/17 mmHg) to give triisobutoxymethylsilane (9.63 g, 90%) as a colorless liquid. ^{1}H NMR (400 MHz, $CDCl_3$, ppm): $\delta = 3.59$ (6H, d, $J = 6.4$ Hz), 1.83 (3H, nonet, $J = 6.4$ Hz), 0.93 (18H, d, $J = 6.8$ Hz), 0.21 (3H, s). ^{13}C NMR (100 MHz, $CDCl_3$, ppm): $\delta = 69.5$, 31.1, 19.2, −7.5. ^{29}Si NMR (100 MHz, $CDCl_3$, ppm): $\delta = -42.9$.

Synthesis of PSQ via the nitrogen flow method

Typically, in a 100 mL four-necked flask equipped with a mechanical stirrer and nitrogen inlet and outlet tubes, triethoxymethylsilane (3.566 g, 20.00 mmol) and ethanol (1.843 g, 40.00 mmol) were stirred at a rotation rate of 150 rpm in an ice/water bath for 10 min under a nitrogen flow rate of 360 mL/min. For the hydrolysis, a solution of 0.3828 g of 6 mol/L HCl and 0.2343 g of water (HCl/monomer molar ratio = 0.105 and water/monomer molar ratio = 1.5) was slowly added dropwise and stirred at 0 °C for 10 min and then at room temperature for an additional 10 min. For the subsequent polycondensation reaction, the reaction mixture was heated for 3 h at 90 °C to afford polymethylsilsesquioxane having ethoxy groups (PSQ-Me (OEt)) as a colorless viscous liquid. The synthesized PSQs were labeled as PSQ-X (OR), where X denotes the organic substituent and OR denotes the residual alkoxy group. PSQ-Me (OEt) was dissolved in THF to prepare a concentration of 20 wt % and stored in a refrigerator. A series of PSQ-Me (OEt) samples with various molecular weights were prepared by changing the amount of 6 mol/L HCl and water (HCl/monomer molar ratio = 0.105 and water/monomer molar ratio = 1.1–1.6). Several co-PSQs were synthesized in a similar manner.

Synthesis of ethoxy-free PSQ

In a 100 mL flask, triethoxyphenylsilane (4.607 g, 20.00 mmol) and ethanol (4.607 g, 100.0 mmol) were added and stirred in an ice/water bath for 10 min. A solution of 0.5834 g of 6 mol/L HCl and 4.968 g of water (3 mmol of HCl and 300.0 mmol of water) was added dropwise and stirred at 0 °C for 10 min and then at room temperature for another 10 min. The reaction mixture was refluxed for 3 h and evaporated under reduced pressure to give PSQ-Ph as a glass-like solid. PSQ-Ph was dissolved in THF to prepare a concentration of 20 wt % and stored in a refrigerator. PSQ-Phe was also synthesized in a similar manner.

Preparation of freestanding gel films

Freestanding films were typically prepared as follows: 1.5 mL of a 20 wt % THF solution of PSQ-Me (OEt) was poured into a PFA vial and heated at 80 and 160 °C for 1 h, respectively. The obtained film was heated at 200 °C for 2 h to give a freestanding gel film.

Chapter 3 Organic–Inorganic Hybrid Thermal Insulation Materials Prepared via Hydrosilylation of Polysilsesquioxane Having Hydrosilyl Groups and Triallylisocyanurate

3.1 Introduction

Among the PSQs, polyhedral oligomeric silsesquioxane (POSS) consisting of a siloxane cage framework and eight organic groups bonded to silicon is widely used as a building block to prepare organic–inorganic hybrid materials because of its excellent thermal and mechanical stability. In this context, POSS has attracted increasing attention in materials chemistry.

Recently, Hamada *et al.* reported that the formation of intramolecular void spaces in an ethylene-bridged PSQ film prepared by the hydrosilylation reaction contributed to the enhancement of its thermal insulation property [43]. Then, with the aim of further improving the thermal insulation property, octavinyl POSS (vinyl-POSS) was used as a crosslinker to prepare a hybrid film containing intramolecular void spaces, finding that increasing the content of intramolecular void spaces around the POSS molecules by increasing the amount of vinyl-POSS enhanced the thermal insulation property [44]. However, the aggregation of POSS molecules due to strong intermolecular interactions hindered the preparation of hybrid films with a high amount of vinyl-POSS (over 20 wt %). In addition, the aggregation of POSS molecules leads to a decrease in the thermal insulation property due to an increase in the thermal conductivity of the hybrid film as a result of the formation of heat conduction pathways. Therefore, we were interested in exploring other crosslinkers with high miscibility to increase the content of intramolecular void spaces in the PSQ film.

Owing to their rigid structure, high polarity, solubility, and miscibility, isocyanurate derivatives are used as building blocks for the preparation of high-performance polymers. For example, crosslinked polymers containing an isocyanurate core exhibit good thermal and mechanical properties [55-57]. In this context, we expected that triallylisocyanurate (TAIC) would be a good candidate as a crosslinker in the PSQ network because of its high miscibility. Furthermore, TAIC could enhance the thermal insulation property and thermal stability of the polymer due to the introduction of a rigid isocyanurate ring and the formation of intramolecular void spaces around it.

In this chapter, with the aim of preventing the formation of aggregates to obtain a highly uniform film with abundant intramolecular void spaces, we designed and prepared hybrid films by the hydrosilylation reaction of hydrodimethylsilylated oligomethylsilsesquioxane (MSQ-SiH) and TAIC. We investigated in detail the effect of the introduction of TAIC in the PSQ network on the thermal insulation property and thermal stability of hybrid films.

3.2 Results and discussion

3.2.1 Preparation of hybrid films by hydrosilylation reaction

In a previous paper, Hamada *et al.* reported the preparation of ethylene-bridged PSQ films via the hydrosilylation reaction of MSQ-SiH and dimethylvinylsilylated oligomethylsilsesquioxane [43]. Compared with polymethylsilsesquioxane films prepared by polycondensation, the ethylene-bridged PSQ films showed low thermal diffusivity and density, which decreased with increasing SiCCSi bond content. This was due to the formation of intramolecular void spaces. Subsequently, we conducted the hydrosilylation reaction of MSQ-SiH and vinyl-POSS, in which the formation of intramolecular void spaces around the POSS molecules enhanced the thermal insulation property [44]. As mentioned in the introduction section of this chapter, the presence of excess POSS units in the hybrid film decreased its transparency; the hybrid film containing 20 wt % POSS units was turbid [44]. The aggregation of POSS molecules leads not only to the decrease in transparency but also to the increase in thermal conductivity due to the formation of POSS-aggregated heat-conducting pathways.

To introduce intramolecular void spaces in the film while preventing the aggregation of crosslinker molecules as described in the Introduction section, we used TAIC as a crosslinker for the hydrosilylation reaction of MSQ-SiH, as shown in Scheme 3.1.

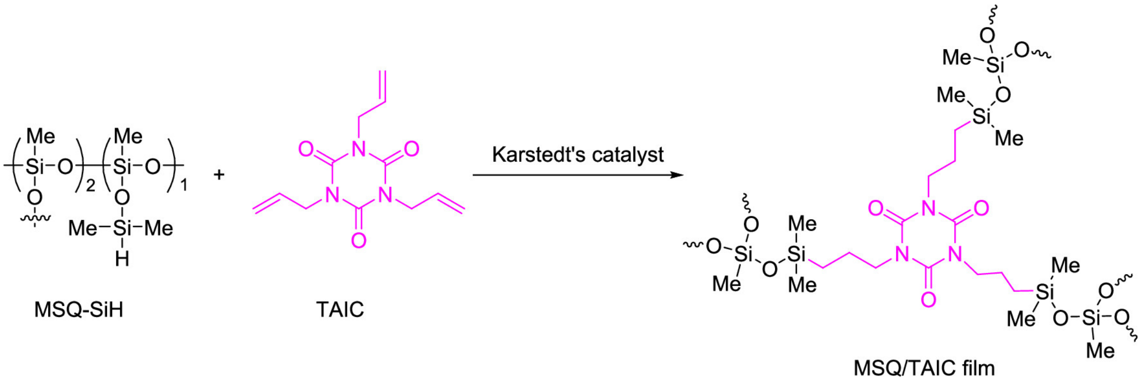

Scheme 3.1 Preparation of MSQ/TAIC hybrid films by the hydrosilylation of MSQ-SiH and TAIC

For the preparation of hybrid films by hydrosilylation, MSQ-SiH was synthesized several times following our previous two-step method to ensure the reproducibility of the reaction [43]. The M_w and M_w/M_n values of MSQ-SiH were 800–1000 and 1.29–1.59, respectively. On the basis of the integral ratio of hydrosilyl group and silylmethyl group in the ^{1}H NMR spectrum of MSQ-SiH, its structure was determined to be $[(MeSiO_{1.5})_2(MeSiO_{1.5}SiMe_2H)_1]_n$, indicating the presence of one hydrosilyl group per three units of $(MeSiO_{1.5})_n$ framework. The hydrosilylation reaction was performed using MSQ-SiH and TAIC according to the procedure described in the Experimental Section. The turbid liquid mixture obtained upon heating up to 140 °C was transformed into a stiff film after heating at 160 °C for 4 h. The hybrid films prepared by the hydrosilylation reaction of MSQ-SiH and TAIC were named as MSQ/TAIC (*x*/*y*), where *x*/*y* indicates the hydrosilyl group/allyl group molar ratio.

Figure 3.1 shows the ATR–FTIR spectra of MSQ-SiH, TAIC, and MSQ/TAIC (1/1). The spectrum of MSQ-SiH shows two characteristic peaks at 2129 and 899 cm^{-1} corresponding to the hydrosilyl group. Absorption peaks at around 1270 and 1100 cm^{-1} ascribable to Si–CH$_3$ and Si–O–Si bonds were also observed. Meanwhile, the spectrum of TAIC shows strong absorption peaks at 1678 cm^{-1} and at 1643, 989, and 926 cm^{-1} due to the carbonyl group and the allyl group, respectively [58]. In the spectrum of MSQ/TAIC (1/1), the peaks corresponding to the hydrosilyl group at 2129 and 899 cm^{-1} and to the allyl group at 1643, 989, and 926 cm^{-1} almost disappeared. Unfortunately, the formation of SiCH$_2$ could not be confirmed by ATR–FTIR due to the overlapping of the SiCH$_2$ peak with those of the Si–CH$_3$ group or the C–N bond. Nevertheless, the ^{13}C solid-state NMR spectrum of MSQ/TAIC (1/1) supported the hydrosilylation reaction between MSQ-SiH and TAIC. As shown in Figure 3.2, the signals of the allyl group of TAIC completely disappeared and new signals attributed to the $SiCH_2CH_2CH_2N$ bond were observed around 14–21 and 43 ppm after the hydrosilylation reaction. In addition, a signal attributable to the carbonyl group in the isocyanurate structure was observed at 148 ppm. These findings clearly indicated that TAIC was introduced into the PSQ network via the formation of $Si–CH_2CH_2CH_2N$ bonds. To confirm the formation of the $SiCH_2CH_2CH_2N$ bond as a crosslink, we evaluated the stability of MSQ/TAIC (1/1) by immersing it in THF. Interestingly, the weight of the hybrid film remained unaltered after 5 days, indicating that TAIC worked as a crosslinker, providing highly networked PSQ structures.

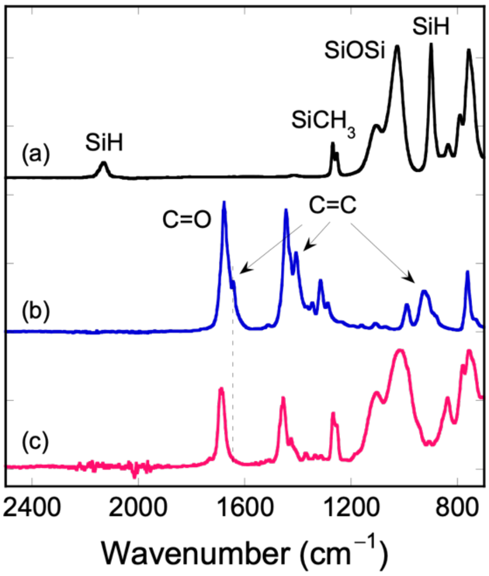

Figure 3.1 ATR-FTIR spectra of (a) MSQ-SiH, (b) TAIC, and (c) MSQ/TAIC (1/1).

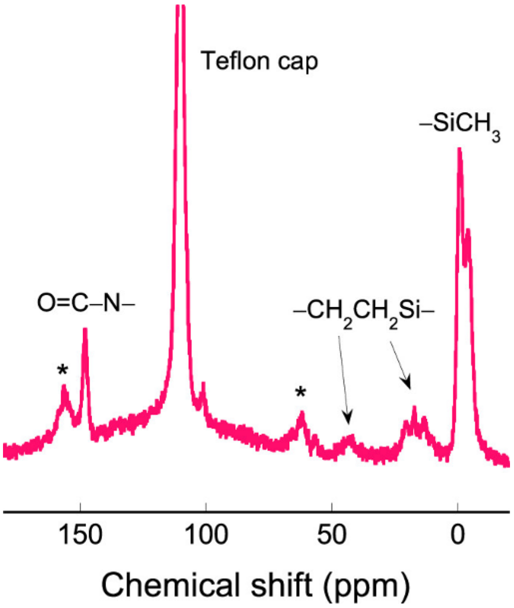

Figure 3.2 ^{13}C solid-state NMR spectrum of an MSQ/TAIC (1/1)) prepared by the hydrosilylation reaction. The asterisks (*) indicate the spinning sidebands.

The ^{29}Si solid-state NMR spectrum of MSQ/TAIC (1/1) provided further structural information. Broad signals were observed at −63.8 and 10.4 ppm, which can be assigned to the T^3 structure and the Si–$CH_2CH_2CH_2N$ unit (Figure 3.3), confirming the successful formation of MSQ/TAIC (1/1) as a crosslinked gel film. However, an unknown signal was observed at −19.4 ppm after the hydrosilylation reaction. The hydrosilyl group in MSQ-SiH has been previously reported to undergo a side reaction with ambient moisture [43, 44]. In this case, the hydrosilyl group could also react with moisture in the presence of the Pt catalyst, forming an Si–O–Si bond by the dehydrogenation reaction of the resultant Si–OH group. This side reaction would furnish an $-Me_2Si–O–SiMe_2-$ (D^2) structure, which could give rise to the signal at −19.4 ppm. In fact, MSQ-SiH formed a gel film upon heating in the presence of the Pt catalyst even in the absence of TAIC. Thus, we obtained a stiff and colorless film, which was named as MSQ film, by subjecting a mixture of MSQ-SiH and Karstedt's catalyst without TAIC to the same heat treatment described for the MSQ/TAIC films. As shown in Figure 3.3, the ^{29}Si solid-state NMR spectrum of the as-prepared MSQ film showed broad signals at −64.4 and −19.4 ppm corresponding to the T^3 and D^2 structures. Besides, a small signal for an unreacted hydrosilyl group was observed at 8.0 ppm. Overall, MSQ-SiH formed the crosslinked gel film via the hydrolysis/dehydrogenation reaction in the presence of the Pt catalyst.

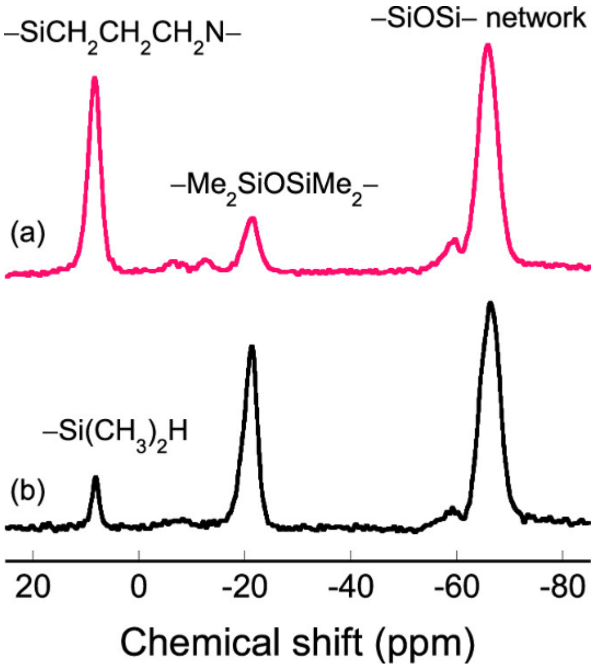

Figure 3.3 ^{29}Si solid-state NMR spectra of (a) MSQ/TAIC (1/1) and (b) MSQ film.

In addition, to investigate the effect of TAIC on the thermal property of the films, we prepared hybrid films having different compositions of MSQ-SiH and TAIC using various MSQ-SiH/TAIC feed molar ratios, i.e., 1:0.25, 1:0.5, 1:0.75, and 1:1.5. All of the obtained MSQ/TAIC (1/0.25–1.15) hybrid films were colorless and transparent.

In our previous paper, a hybrid film containing POSS units showed high surface hardness stemming from the effect of POSS as a nanofiller; however, the amount of POSS molecules that can be introduced was limited by aggregation [44]. In contrast, the high miscibility of TAIC allowed introducing a high amount of TAIC molecules. Furthermore, MSQ/TAIC exhibited high flexibility. Interestingly, the flexibility of hybrid films increased with increasing amount of TAIC, which indicates that the property of hybrid films can be tuned by controlling the TAIC content. Meanwhile, the surface property of the hybrid films did not change upon the introduction of TAIC, and the contact angles of the MSQ film, MSQ/TAIC (1/1), and MSQ/TAIC (1/0.5) were

89–90°. This is owing to the hydrophobic nature of the methyl group of the polymethylsilsesquioxane backbone on the surface of the films.

3.2.2 Thermal insulation property of hybrid films prepared by hydrosilylation reaction

As we previously reported, the crosslinked structure of ethylene-bridged PSQ films created void spaces and reduced the thermal diffusivity of the films [43, 44]. To investigate the effect of the intramolecular void spaces formed around the TAIC molecules, we prepared hybrid films having different amounts of TAIC and measured their thermal diffusivities. The thermal diffusivity of the MSQ film prepared by the coupling reaction of the hydrosilyl group was 1.44×10^{-7} m^2/s (Table 3.1), which was considerably higher than that of the PSQ films prepared via the sol–gel reaction. The previously reported PSQ film prepared using oligomethylsilsesquioxane containing no ethoxy groups exhibited a high thermal diffusivity of 1.36×10^{-7} m^2/s due to the formation of a highly crosslinked network structure [43, 44]. As shown in Figure 3.3, the coupling reaction of the hydrosilyl group in MSQ-SiH effectively proceeded to form a highly crosslinked network structure, enabling the formation of the heat conduction pathway. However, the introduction of TAIC into the PSQ network greatly decreased the thermal diffusivity. Compared with the MSQ film, the thermal diffusivity decreased significantly by adding TAIC into the PSQ network. Thus, MSQ/TAIC (1/0.25) showed a thermal diffusivity of 1.14×10^{-7} m^2/s. Moreover, decreasing the MSQ-SiH/TAIC molar ratio from 1:0.25 to 1:1.5 led to a further decrease in the thermal diffusivity of the hybrid film down to 1.01×10^{-7} m^2/s (Table 3.1 and Figure 3.4). This may be due to the formation of voids around TAIC molecules.

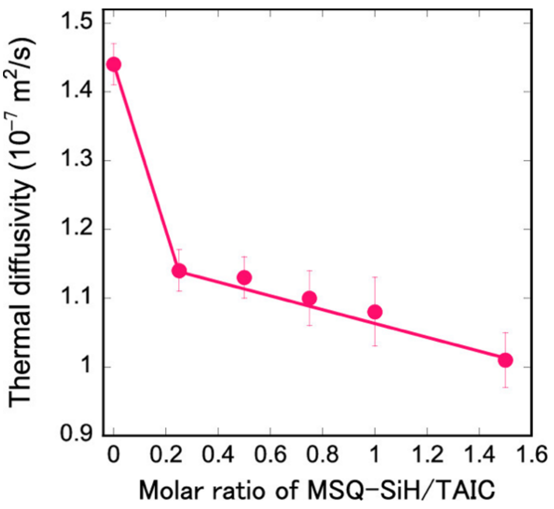

Figure 3.4 Influence of the amount of TAIC in the polysilsesquioxane film on the thermal diffusivities of isocyanurate ring-containing hybrid films prepared from MSQ-SiH and TAIC.

Table 3.1. Thermal diffusivity and density of PSQ films with and without isocyanurate rings

	Thermal diffusivity (m^2/s)[a]	Density (g/cm^3)
MSQ film	1.44×10^{-7}	1.18
MSQ/TAIC (1/0.25) film	1.14×10^{-7}	1.18
MSQ/TAIC (1/0.5) film	1.13×10^{-7}	1.20
MSQ/TAIC (1/0.75) film	1.10×10^{-7}	1.19
MSQ/TAIC (1/1) film	1.08×10^{-7}	1.19
MSQ/TAIC (1/1.5) film	1.01×10^{-7}	1.18
PSQ/TESIC film	1.25×10^{-7}	1.28

[a] The thermal diffusivity values are the average of 21 independent measurements. TESIC = tris(triethoxysilylpropyl)isocyanurate.

To demonstrate the convenience of using MSQ-SiH to prepare the MSQ/TAIC hybrid films by hydrosilylation reaction, we prepared a PSQ film containing the isocyanurate ring by the polycondensation reaction of a polymethylsilsesquioxane having a molecular weight similar to that of MSQ-SiH (M_w = 1200) and TESIC as a control experiment. First, we synthesized the polymethylsilsesquioxane by the sol–gel reaction of triethoxymethylsilane according to Chapter 2 and TESIC by the hydrosilylation reaction of TAIC with triethoxysilane (Scheme 3.2). The ^{1}H NMR and HRMS of the as-prepared TESIC confirmed that it was obtained in high purity by simply removing the solvent from the reaction mixture under high vacuum. To obtain a molar ratio of polymethylsilsesquioxane and TESIC similar to that of MSQ/TAIC (1/1), we heated a mixture of polymethylsilsesquioxane and 30 wt % tris(triethoxysilylpropyl)isocyanurate at 80, 100, 120, and 140 °C for 1 h, respectively, and at 160 °C for 4 h in a PFA vial. However, in contrast with the MSQ/TAIC films prepared by hydrosilylation, the film was still not cured at 160 °C and required further heating at 200 °C for 3 h to form a colorless and transparent PSQ/TESIC film. The chemical structure of PSQ/TESIC was investigated using ATR–FTIR and ^{13}C solid-state NMR spectroscopic analyses. Although the ATR–FTIR spectra of PSQ/TESIC provided only limited information, useful information was extracted from the ^{13}C solid-state NMR of PSQ/TESIC prepared via polycondensation. Specifically, strong signals attributable to the remaining ethoxy group were observed at 18 and 58 ppm, along with the signal owing to the $SiCH_3$ group and small signals ascribable to the $SiCH_2CH_2CH_2N$ bond and the carbonyl group in the isocyanurate structure (Figure 3.5). The PSQ/TESIC film prepared by polycondensation showed a thermal diffusivity of 1.25×10^{-7} m^2/s, which was higher than that of the MSQ/TAIC hybrid films regardless of the amount of TAIC (Table 3.1).

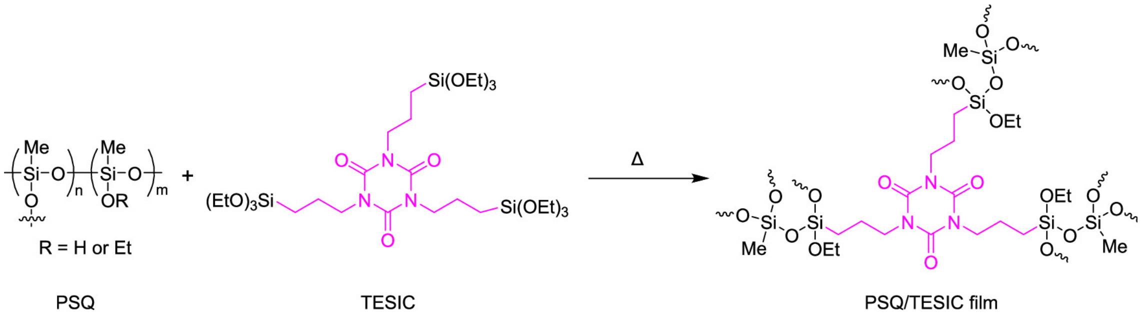

Scheme 3.2 Preparation of PSQ/TESIC by Polycondensation Reaction

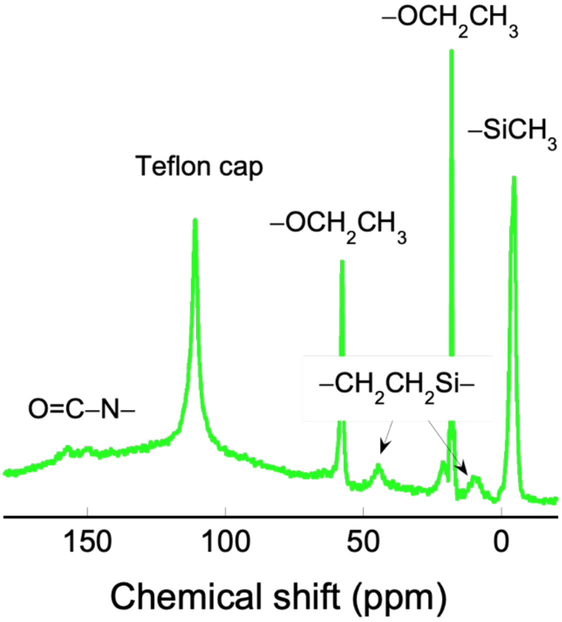

Figure 3.5 ^{13}C solid-state NMR spectrum of PSQ/TESIC prepared by the polycondensation reaction of a polymethylsilsesquioxane (M_w = 1200) and TESIC.

To elucidate the reason for the decrease in the thermal diffusivity of hybrid films with the addition of TAIC, we performed a positron annihilation lifetime analysis of the MSQ film and the MSQ/TAIC (1/1) hybrid film because the small size of the expected intramolecular void spaces hindered the analysis via N_2 adsorption–desorption isotherms. Three components were separated, and the longest lifetime was set as the pick-off annihilation of *ortho*-positronium. Then, we obtained the probability density function of the annihilation rate using a numerical Laplace inversion technique (Figure 3.6) [59]. Surprisingly, MSQ/TAIC (1/1) exhibited a lower peak position and a shorter lifetime (2.58 ns) than the MSQ film (3.29 ns), as shown in Table 3.2. The volume of free-volume holes (R) for MSQ and MSQ/TAIC (1/1) estimated using the Tao–Eldrup equation was 0.23 and 0.15 nm^3, respectively [46, 47]. Although we expected that the thermal diffusivities of the MSQ/TAIC hybrid films decreased as a result of the formation of intramolecular void spaces around the TAIC molecules, the positron annihilation lifetime analysis showed the opposite results. In fact, the intramolecular void spaces of MSQ/TAIC (1/1) were smaller than those of the MSQ film, as shown in Table 3.2. In the hybrid film containing POSS units, the three-dimensional structure of the POSS molecules favored the formation of intramolecular void spaces, which enhanced the thermal insulation property. The density of the hybrid film containing POSS molecules decreased with the increase in intramolecular void spaces [44]. In the case of MSQ/TAIC (1/1), the isocyanurate ring has a planar structure that could hinder the formation of intramolecular void spaces around the TAIC molecules. Furthermore, unlike the ethylene-bridged structure, the longer and more flexible propylene chain is less conducive to the formation of intramolecular void spaces. Similarly, a fully atomistic molecular dynamics (MD) simulation suggested that the number of intramolecular void spaces did not increase by the introduction of TAIC molecules into the PSQ network (Figure 3.7). Indeed, the densities of the MSQ/TAIC films were similar regardless of the amount of TAIC molecules, as shown in Table 3.1, even though the reason for this is unclear. Therefore, the decrease in the thermal diffusivity of the MSQ/TAIC hybrid films can be attributed to the nature of the TAIC units rather than to the formation of intramolecular void spaces. In addition, we ruled out the formation of cracks and dimples as a possible reason for the decrease in thermal diffusivity by performing HR-TEM measurements (Figure 3.8). A similar behavior was observed in Chapter 2 for a polyphenylsilsesquioxane film; namely, its thermal diffusivity was lower than that of other PSQ films. Although the origin of this phenomenon is unclear at this stage and it is difficult to explain the decrease in the thermal diffusivity as a result of the nature of the TAIC unit, the TAIC molecule might also have a role in preventing the heat conduction on the basis of the following speculations: (i) organic crosslinking units such as C–C and C–N bonds are less prone to conduct heat than Si–O–Si bonds, (ii) the unreactive allyl group blocks the heat conduction because of the presence of noncovalent bonds between the polymer chains, and (iii) the cyclic structure of the isocyanurate ring holds the heat. Further studies are required to gain more insight into this phenomenon.

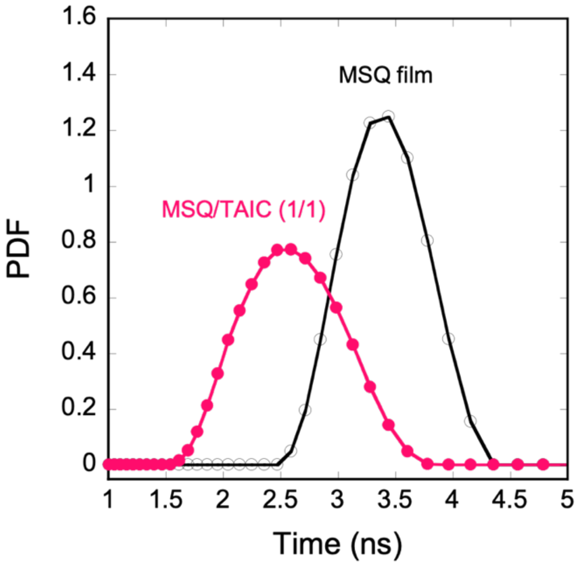

Figure 3.6 Probability density function (PDF) of the ortho-positronium lifetime in MSQ film and MSQ/TAIC (1/1).

Table 3.2. Lifetime (τ_3), relative intensity (I_3), and radius of free-volume holes for the annihilation of *ortho*-positronium in MSQ film and MSQ/TAIC (1/1)

	Lifetime (τ_3)	I_3 (%)	V (nm^3)[a]
MSQ film	3.29 ± 0.01	38	0.23
MSQ/TAIC (1/1) film	2.58 ± 0.01	35	0.15

[a] The radius and volume of free-volume holes were estimated using the Tao–Eldrup equation.

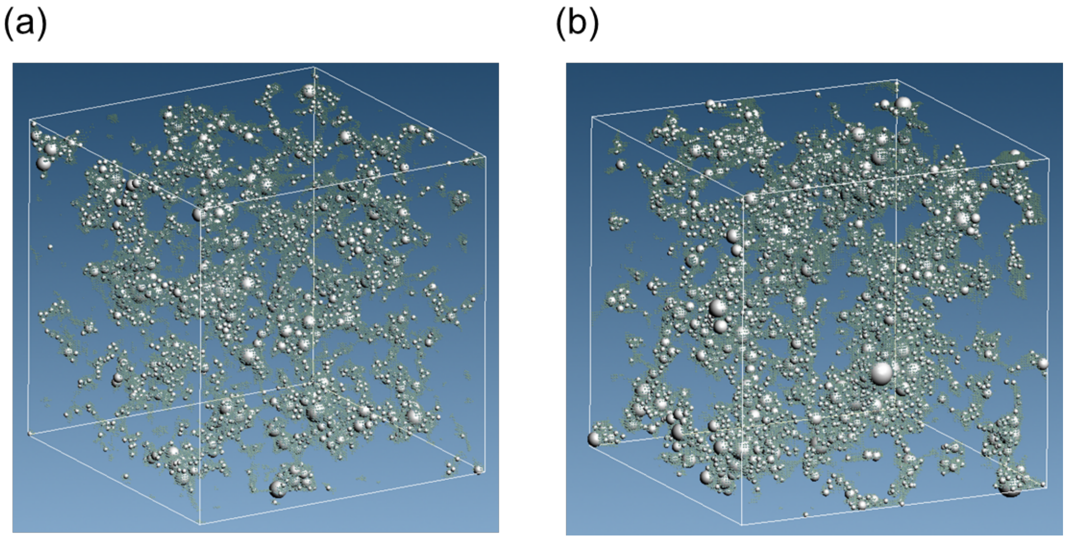

Figure 3.7 Intramolecular voids (free volume) in (a) a polysilsesquioxane film without isocyanurate and (b) an isocyanurate ring-containing polysilsesquioxane film calculated by full atomic molecular dynamics. J-OCTA/VSOP was used to calculate the crosslinked structure of the polymers. We divided the cell lattice of the molecular models into subcells in 0.4 Å increments and placed a test particle having a diameter of 0.4 Å in the center of each subcell to identify those which contained a void, considering only the Lennard–Jones interaction between the polymer molecules. We also filled the subcells containing voids with virtual spheres and evaluated the size of the free volume. Only the virtual spheres with free volume are shown in the figure.

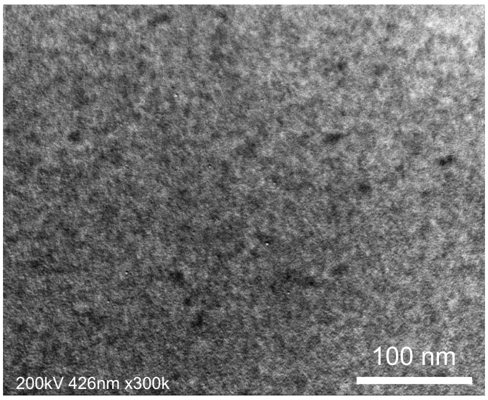

Figure 3.8 High-resolution transmittance electron microscopy image of a cross-section of MSQ/TAIC (1/1).

3.2.3 Thermal stability of hybrid films prepared by hydrosilylation reaction

To investigate the effect of the rigid isocyanurate structure on the thermal stability of the films, we evaluated the thermal stabilities of MSQ/TAIC (1/1) and MSQ/TAIC (1/0.5) by TG/DTA, along with those of the MSQ film and PSQ/TESIC for comparison (Figure 3.9). As shown in Table 3.3, the MSQ film exhibited high thermal stability with a 5% weight loss temperature (T_d^5) and 10% weight loss temperature (T_d^{10}) of 472 and 724 °C, respectively. Surprisingly, the MSQ film exhibited an extremely high ceramic yield of 89% at 800 °C. In contrast, MSQ/TAIC (1/1) and MSQ/TAIC (1/0.5) showed lower T_d^5 and T_d^{10} (380–444 and 427–473 °C, respectively). Unlike the siloxane-based cyanate ester elastomer prepared via the hydrosilylation reaction of hydride-terminated siloxane and 2,4,6-tris(allyloxy)-1,3,5-triazine [60], the introduction of TAIC into the PSQ network decreased the thermal stability. However, the T_d^5 and T_d^{10} of MSQ/TAIC (1/1) and MSQ/TAIC (1/0.5) were considerably higher than those of organic polymer-based thermal insulation materials, such as polyurethane and expanded polystyrene [61]. In addition, the thermal stability of the MSQ/TAIC hybrid films was higher than that of TAIC-containing polyacrylate and polymethyacrylate, which exhibited T_d^5 values of only 230–280 °C [57], and hybrid materials composed of poly(*N*-allyimaleimide-*co*-*N*-(2-ethylhexyl)maleimide-*co*-diisobutylene) containing TAIC and the PSQ structure reported by Matsumoto *et al.* (T_d^5 = 320 °C–370 °C) [30].

Meanwhile, the thermal stability of PSQ/TESIC (T_d^5 = 246 °C and T_d^{10} = 282 °C) was significantly lower than that of MSQ/TAIC (1/1) because of the decomposition of the remaining ethoxy groups (Figure 3.9 and Table 3.3). Taken together, these results demonstrate that MSQ-SiH without ethoxy groups is a suitable oligomer for preparing hybrid materials with high thermal stability.

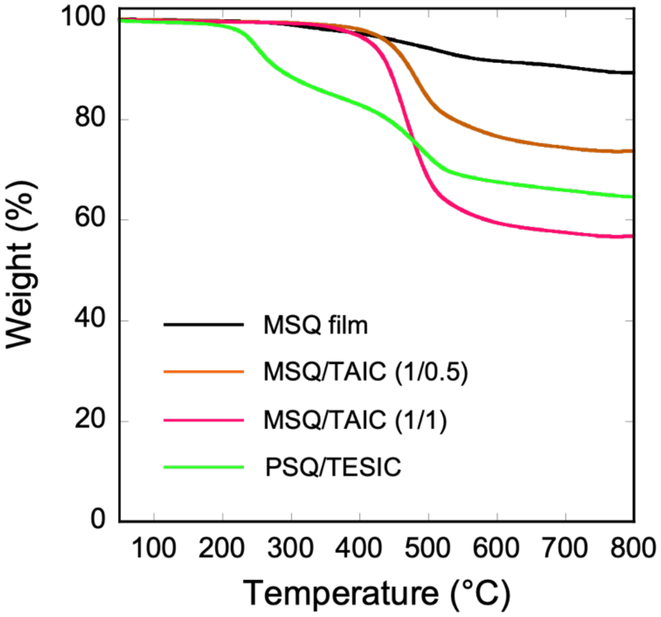

Figure 3.9 Thermogravimetric profiles of MSQ, MSQ/TAIC (1/0.5) and MSQ/TAIC (1/1), and PSQ/TESIC measured at a heating rate of 10 °C/min under nitrogen.

Table 3.3 Thermal stability of MSQ film, MSQ/TAIC (1/0.5) and MSQ/TAIC (1/1), and PSQ/TESIC

	T_d^5 (°C)[a]	T_d^{10} (°C)[a]	residue at 800 °C (%)[a]
MSQ film	472	724	89
MSQ/TAIC (1/0.5)	444	473	74
MSQ/TAIC (1/1)	380	427	57
PSQ/TESIC	246	282	65

[a] Measured at a heating rate of 10 °C/min under a nitrogen flow of 100 mL/min.

3.3 Conclusions

MSQ/TAIC hybrid films containing isocyanurate rings were prepared by the hydrosilylation reaction of MSQ-SiH and TAIC in the presence of Karstedt's catalyst. ATR–FTIR and ^{13}C and ^{29}Si solid-state NMR spectra confirmed that the hydrosilylation reaction of MSQ-SiH with TAIC proceeded to form MSQ/TAIC hybrid films, along with the side reaction of the hydrosilyl group with moisture. When MSQ/TAIC (1/1) was immersed in THF, the film weight remained unchanged even after 5 days, indicating the formation of a crosslinked structure. The obtained MSQ/TAIC hybrid films were colorless, transparent, and stiff irrespective of the amount of TAIC in the PSQ network. The thermal diffusivity of the MSQ/TAIC hybrid films decreased from 1.14×10^{-7} to 1.01×10^{-7} m^2/s with increasing amount of TAIC in the molar ratio range of 1/0.25–1/1.15 and was lower than that of a TAIC-free MSQ film prepared by the coupling reaction of MSQ-SiH (1.44×10^{-7} m^2/s) and a PSQ/TESIC film prepared by polycondensation (1.25×10^{-7} m^2/s). A positron annihilation lifetime analysis indicated that the nature of the isocyanurate ring, rather than the formation of intramolecular void spaces, was responsible for the decrease in thermal diffusivity. Although the T_d^5 and T_d^{10} values of the MSQ film (472 and 724 °C, respectively) were higher than those of the MSQ/TAIC films, the T_d^5 and T_d^{10} values of MSQ/TAIC (1/1) and MSQ/TAIC (1/0.5) (380–444 and 427–473 °C, respectively) were higher than those of PSQ/TESIC ($T_\mathrm{d}^5 = 246$ °C and $T_\mathrm{d}^{10} = 282$ °C) and previously reported TAIC-containing polymer films, which demonstrates that using MSQ-SiH without ethoxy groups as an oligomer is a promising strategy toward hybrid materials with high thermal stability.

3.4 Experimental

Materials

Triethoxymethylsilane, triethoxysilane, and TAIC were purchased from Tokyo Chemical Industry Co., Ltd. (Tokyo, Japan) and used as received. Toluene (super dehydrated), THF (super dehydrated), ethanol (super dehydrated), and 6 mol/L hydrochloric acid (HCl) were purchased from FUJIFILM Wako Pure Chemical Co., Ltd. (Osaka, Japan). Platinum(0)-1,3-divinyl-1,1,3,3-tetramethyldisiloxane complex solution in xylene (Karstedt's catalyst) was purchased from

Sigma-Aldrich and used as received. Water was purified using a Millipore Milli-Q UV system and had a resistance of 18.2 MΩ·cm and a total organic carbon content of <10 ppb.

Characterizations

^{1}H, ^{13}C, and ^{29}Si NMR measurements were performed on a Varian 500 MHz spectrometer. The samples were dissolved in $CDCl_3$, and residual chloroform or tetramethylsilane was used as an internal standard for chemical shift referencing. ^{13}C and ^{29}Si solid-state NMR measurements were performed on a Varian 600 MHz spectrometer. Attenuated total reflection Fourier transform infrared (ATR–FTIR) spectra were recorded on a Shimadzu IR Affinity-1 spectrometer equipped with an ATR unit. High-resolution mass spectra (HRMS) were recorded on a Thermo Scientific LTQ Orbitrap XL hybrid Fourier transform mass spectrometer using electrospray ionization. The contact angle of the film was measured using a KYOWA DM 300 contact angle meter; the measurements were repeated five times, and the average contact angle was calculated. Thermogravimetry/differential thermal analysis (TG/DTA) was performed on an SII EXSTAR TG-DTA 6200 thermal analyzer at a heating rate of 10 °C/min under a nitrogen flow of 100 mL/min. Thermal diffusivity measurements were conducted on an ai-phase Mobile M3 type 1 system. The measurements were repeated 21 times and the averaged thermal diffusivity was calculated excluding extreme maximum and minimum values. The density of the films was determined via the Archimedes method by measuring the film weight in air and water. Positron lifetime measurements were performed using a system based on a digital oscilloscope according to Chapter 2. High-resolution transmittance electron microscopy (HR-TEM) was performed on a JEOL JEM 2011 microscope operating at 200 kV. For the TEM sample preparation, the film was embedded in an epoxy resin and the cross-section of the film was sliced with a microtome.

Synthesis of MSQ-SiH

MSQ-SiH was synthesized via a two-step reaction. First, the sol–gel reaction of triethoxymethylsilane was conducted using excess HCl and water, and the capping reaction was then performed using chlorodimethylsilane. The detailed synthesis procedure for MSQ-SiH was described in previous chapter

Synthesis of Polymethylsilsesquioxane

Polymethylsilsesquioxane was prepared as in Chapter 2. Briefly, triethoxymethylsilane (3.57 g, 20.0 mmol) and ethanol (1.84 g, 40.0 mmol) were added into a 100 mL four-necked flask equipped with a mechanical stirrer and a nitrogen inlet and outlet. The resulting solution was cooled in an ice bath for 10 min under a nitrogen stream of 360 mL/min. After adding 6 mol/L HCl (0.383 g) and water (0.0902 g) to achieve a water/triethoxymethylsilane ratio of 1.1 while stirring (150 rpm), the reaction mixture was stirred at 0 °C and room temperature for 10 min. Finally, the reaction mixture was heated at 90 °C for 3 h to conduct the polycondensation reaction, which afforded polymethylsilsesquioxane as a slightly viscous liquid (1.55 g).

Synthesis of Tris(3-triethoxysilylpropyl)isocyanurate (TESIC)

TAIC (2.23 g, 8.95 mmol) and triethoxysilane (5.12 g, 31.2 mmol) were dissolved in 5 mL of toluene. After adding a few drops of Karstedt's catalyst in xylene, the reaction mixture was stirred for 2 h at 110 °C. Toluene and excess triethoxysilane were evaporated under vacuum to afford TESIC (6.55 g, 99%) as a colorless liquid, which was used for the polycondensation reaction without any purification. ^{1}H NMR (500 MHz, $CDCl_3$, ppm): $\delta = 0.63$ (6H, t, CH_2Si, $J = 8.5$ Hz), 1.21 (27H, t, CH_2CH_3, $J = 7.0$ Hz), 1.69–1.76 (6H, m, $CH_2CH_2CH_2$), 3.81 (18H, q, OCH_2CH_3, $J = 7.0$ Hz); ^{13}C NMR (125 MHz, $CDCl_3$, ppm): $\delta = 7.6, 18.2, 21.3, 45.3, 58.4, 148.8$; ^{29}Si NMR (100 MHz, $CDCl_3$, ppm): $\delta = -46.2$; and HRMS (ESI, positive): calcd for $C_{30}H_{63}O_{12}N_3NaSi_3$ $m/z = 764.36117$ [M + Na^+], found $m/z = 764,36102$.

Preparation of Hybrid Films by the Hydrosilylation Reaction of MSQ-SiH and TAIC

The hybrid films were prepared according to our previous paper. (17,18) Typically, MSQ-SiH (0.401 g) and TAIC (0.139 g) were added into a plastic cup and mixed using a rotation/revolution vacuum mixer at 1600 rpm for 10 min. Then, 10 wt % Karstedt's catalyst solution (10-times diluted with toluene) was added and mixed again at the same condition. The obtained mixture was either transferred to a PFA vial with an inner diameter of 18.4 mm or coated on a Teflon-coated substrate using an applicator with a gap size of 300–500 μm, and then heated at 80, 100, 120, and 140 °C for 1 h at each temperature and at 160 °C for 4 h. Depending on the method used, the obtained gel film was taken from the PFA vial or peeled off from the Teflon-coated substrate.

Preparation of Hybrid Films by the Polycondensation Reaction of Polymethylsilsesquioxane with TESIC

Into a PFA vial with an inner diameter of 18.4 mm, 0.604 g of 50 wt % polymethylsilsesquioxane solution in THF and 0.101 g of TESIC were added and heated at 80, 120, and 140 °C for 1 h, respectively. Finally, to obtain the hybrid film, the highly viscous liquid was heated in the PFA vial at 160 °C for 4 h and at 200 °C for 3 h.

Chapter 4 Double-Decker Silsesquioxane-Grafted Polysilsesquioxane Hybrid Films as Thermal Insulation Materials

4.1 Introduction

In Chapter 3, we attempted to create intramolecular void spaces in the PSQ film by using TAIC as a cross-linking agent. Moreover, the high miscibility of TAIC with the PSQ network allowed introducing a high amount of TAIC. Unfortunately, although the introduction of TAIC enhanced the thermal insulating property of the PSQ film via another heat conduction mechanism not attributed to the formation of intramolecular void spaces, its thermal stability was reduced.

In our quest for an ideal crosslinker that creates intramolecular void spaces without aggregation while maintaining high thermal stability and transparency, we turned our attention to double-decker silsesquioxane (DDSQ), which exhibits a unique structure composed of two tetraphenylcyclotetrasiloxanes linked via siloxane bonds bearing two reactive functional groups such as hydrosilyl and vinyl groups [62, 63]. DDSQ is used as the starting monomer for the preparation of hybrid polymers because it exhibits high thermal stability and mechanical properties similar to those of POSS molecules. For example, polyimide-, polyurethane-, and polysiloxane-based materials containing DDSQ structures with enhanced thermal stability and mechanical property have been synthesized [64-66]. Additionally, DDSQ-containing polymers exhibit relatively good solubility in common organic solvents and generally form transparent films due to their high miscibility with the base polymers.

In this study, hybrid polymer films containing DDSQ were prepared via the hydrosilylation reaction of MSQ-SiH and DDSQ with two vinyl groups to prevent aggregation and improve the thermal insulation property and thermal stability. The effect of the DDSQ structure in the PSQ film on the thermal insulation property and the thermal stability compared with POSS-containing PSQ films was investigated.

4.2 Results and discussion

4.2.1 Preparation of DDSQ-grafted PSQ films via a two-step reaction

As reported in our previous paper, POSS-containing hybrid films were successfully prepared via the hydrosilylation reaction of MSQ-SiH and vinyl-POSS in a vacuum mixer [44]. Owing to the formation of Si–CH_2CH_2–Si bonds, the obtained hybrid films containing 5–10 wt% of POSS molecules were colorless and transparent stiff films. Interestingly, the thermal diffusivities of the hybrid films decreased with an increase the POSS amount in the range of 5–20 wt % as a result of the formation of intramolecular void spaces around the POSS molecules. However, we previously found that under the reaction conditions, the dehydrogenation reaction between the hydrosilyl group in MSQ-SiH and trace moisture also occurred in the presence of the Platinum (Pt) catalyst, competing with the hydrosilylation reaction and forming Si–O–Si bonds . Therefore, to avoid the undesired dehydrogenation reaction, the hydrosilylation reaction between MSQ-SiH and vinyl-functionalized DDSQ (vinyl-DDSQ) was conducted according to the two-step process shown in Scheme 4.1. First, the hydrosilylation reaction of MSQ-SiH and vinyl-DDSQ was conducted in solution under a nitrogen atmosphere to induce the formation of Si–CH_2CH_2–Si bonds in the absence of moisture, thereby creating the desired intramolecular void spaces. Then, the dehydrogenation reaction was conducted in the film state to afford a cross-linked gel film via the formation of Si–O–Si bonds.

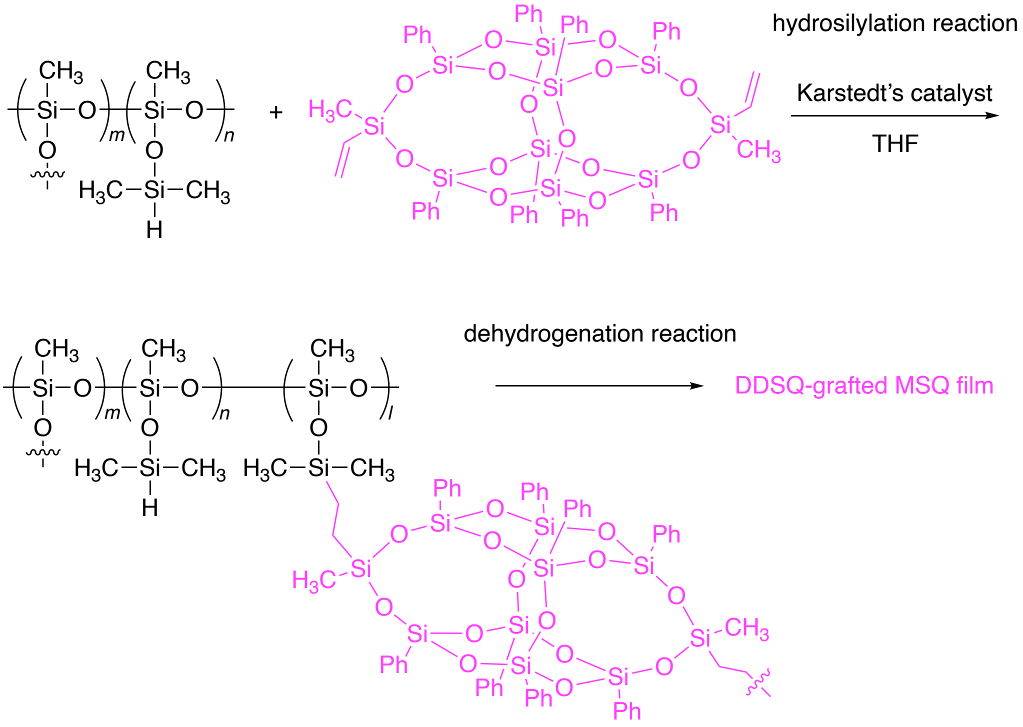

Scheme 4.1 Preparation of a double-decker silsesquioxane (DDSQ)-grafted polysilsesquioxane (PSQ) film via a two-step reaction between MSQ-SiH and vinyl-DDSQ.

To prepare DDSQ-grafted PSQ, MSQ-SiH with $M_w = 1100$ and $M_w/M_n = 1.30$ was reacted with 15 mol% vinyl-DDSQ in THF in the presence of Karstedt's catalyst, and the reaction progress was monitored by ^{1}H NMR spectroscopy. In the ^{1}H NMR spectrum of a mixture of MSQ-SiH and vinyl-DDSQ before adding the Pt catalyst, distinct signals of the vinyl groups of vinyl-DDSQ and the hydrosilyl groups of MSQ-SiH were observed at 5.91–6.19 ppm and 4.72 ppm, respectively (Figure 4.1). The vinyl group of vinyl-DDSQ was almost consumed within 1 h, whereas a signal corresponding to the hydrosilyl group was still observed at 4.72 ppm. New peaks attributed to the Si–CH_2CH_2–Si bonds formed via hydrosilylation were observed at 0.53 and 0.62 ppm. This indicates that the hydrosilylation reaction between the vinyl group of vinyl-DDSQ and the hydrosilyl group of MSQ-SiH occurred preferentially over the dehydrogenation reaction in the absence of moisture. The hydrosilyl group remained even after 3–5 h and gel formation was not observed in the solution. Finally, to ensure the grafting of DDSQ molecules into the PSQ backbone, the reaction was allowed to continue overnight. Then, the solvent was removed in an evaporator, affording DDSQ-grafted PSQ as a viscous and colorless oil. Additionally, ^{29}Si NMR spectrum of DDSQ-grafted PSQ containing 15 mol% DDSQ molecules provided useful information concerning the grafting of DDSQ (Figure 4.2). The peaks at around −64.6 ppm and −78.3∼−79.5 ppm, corresponding to the T^3 structure in MSQ-SiH and the main backbone of DDSQ, were mainly observed, along with the remaining hydrosilyl group at −5.4 ppm and the formed the Si–CH_2CH_2–Si bonds at −31.36 and −31.44 ppm. Therefore, the grafting degree of DDSQ was controlled by the feed of vinyl-DDSQ and the remaining hydrosilyl group makes it possible to perform the dehydrogenation reaction for the preparation of film. However, the small peak was also observed at −17.0 ppm. This might be due to the side reaction, namely, the dehydrogenation reaction of a partial hydrosilyl groups with the ambient moisture underwent the formation of Si–O–Si bond during the process of removal of solvent.

The M_w and M_w/M_n values were estimated to be 4,000 and 2.39 by GPC after the hydrosilylation reaction of MSQ-SiH with 15 mol% vinyl-DDSQ. The molecular weight of DDSQ-grafted PSQ increased with increasing the amount of vinyl-DDSQ, and the M_w and M_w/M_n of DDSQ-grafted PSQ containing 25 mol% DDSQ increased to 13,700 and 3.27, respectively. The same result was obtained upon adding further vinyl-DDSQ to the overnight reaction.

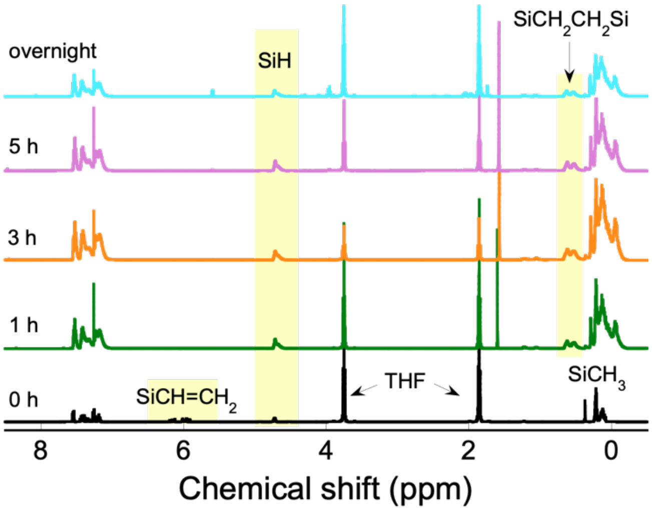

Figure 4.1 ^{1}H NMR spectra of the time course of the hydrosilylation reaction between MSQ-SiH and vinyl-DDSQ in solution under a nitrogen atmosphere. The spectra were recorded by diluting $CDCl_3$ aliquots taken from the reaction mixture at the specified time points.

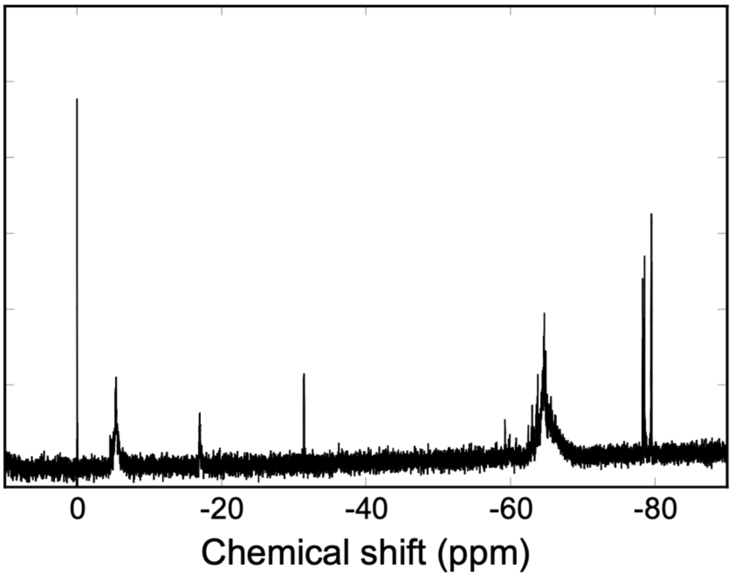

Figure 4.2 ^{29}Si NMR spectrum of DDSQ-grafted PSQ containing 15 mol% DDSQ in $CDCl_3$.

Next, to prepare the hybrid film, the obtained DDSQ-grafted PSQ was poured into a poly PFA vial with an inner diameter of 18.4 mm and heated in an oven under air atmosphere at 80, 100, 120, and 140 °C for 1 h at each temperature and finally at 160 °C for 4 h for the dehydrogenation reaction to proceed. The FT-IR spectrum of the product obtained after this treatment revealed the complete disappearance of the characteristic peaks of the hydrosilyl group at 2100 and 900 cm^{-1}, which were observed in the FT-IR spectrum of DDSQ-grafted PSQ before the hydrogenation reaction (Figure 4.3). Although the newly formed Si–O–Si bonds could not be identified in the FT-IR spectrum because their signal overlapped with the peaks of Si–O–Si bonds in the PSQ backbone, the progress of the dehydrogenation reaction was supported by the change in the appearance of DDSQ-grafted PSQ from a viscous product to a stiff gel, as described in our previous report [44].

To investigate the influence of the DDSQ structure on the thermal properties of the hybrid film, DDSQ-grafted PSQ with different DDSQ contents in the range of 5–25 mol% were prepared via the hydrosilylation reaction between MSQ-SiH and vinyl-DDSQ. Colorless and transparent DDSQ-grafted PSQ films were obtained in all cases, regardless of the DDSQ content. In the case of POSS-containing hybrid films, when the POSS amount exceeded 20 wt%, the hybrid film became turbid even after the formation of $Si–CH_2CH_2–Si$ bonds via hydrosilylation, as reported in our previous study [44], because POSS molecules tend to aggregate in the film state. In contrast, the eight phenyl groups on the silicon atoms of the DDSQ molecule enhanced its solubility, and their steric hindrance prevents the aggregation of DDSQ in the PSQ network. As a result, the obtained DDSQ-grafted PSQ films showed high transparency even for a DDSQ amount of 25 mol%. To obtain the morphological information of hybrid film containing the POSS molecules, DDSQ-grafted PSQ containing 25 mol% DDSQ molecules was casted on the silicon wafer, and it was heated at the same conditions for the atomic force microscope (AFM) measurement. DDSQ-grafted PSQ film containing 25 mol% DDSQ molecules showed the smooth surface morphology (Figure 4.4). This means that DDSQ molecules were uniformly introduced into PSQ network via the covalent bond without aggregation. Furthermore, the pencil hardness of the POSS-containing hybrid films exhibited an excellent hardness of 6H and was higher than that of a PSQ film (2H) without POSS prepared via the polycondensation reaction of oligomethylsilsesquioxane (MSQ-OH) [44]. The rigid POSS improved the hardness of the hybrid film as a filler via the formation of covalent bonds. However, contrary to expectations, the hardness of the hybrid films containing DDSQ decreased with an increase the vinyl-DDSQ content from 5 to 25 mol%.

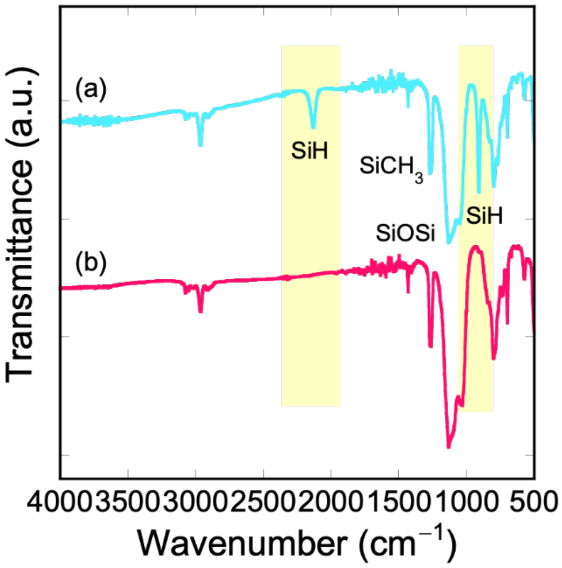

Figure 4.3 FT-IR spectra of (a) DDSQ-grafted PSQ containing 15 mol% vinyl-DDSQ (before the dehydrogenation reaction) and (b) DDSQ-grafted PSQ film containing 15 mol% vinyl-DDSQ (after the dehydrogenation reaction).

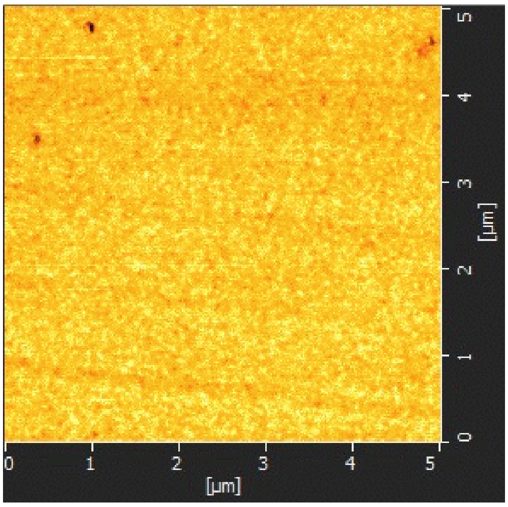

Figure 4.4 Atomic force microscope (AFM) image of DDSQ-grafted PSQ film containing 25 mol% DDSQ on the silicon wafer.

4.2.2 Thermal diffusivity of the DDSQ-grafted PSQ films

We previously reported that the ethylene-bridged structure prepared via hydrosilylation reaction provided intramolecular void spaces around the POSS molecule that enhanced the thermal insulation property [43, 44]. Thus, a POSS-free PSQ film prepared by polycondensing MSQ-OH exhibited a thermal diffusivity of 1.36×10^{-7} m^2/s [43, 44], whereas that of an ethylene-bridged PSQ film prepared via the hydrosilylation reaction between MSQ-SiH and dimethylvinylsilylated MSQ (MSQ-SiVi) was 1.15×10^{-7} m^2/s [43]. Surprisingly, the thermal diffusivity decreased from 1.21×10^{-7} to 1.01×10^{-7} m^2/s on introducing POSS molecules (5–20 wt%) [44], indicating that the introduction of POSS improved the thermal insulating properties of the PSQ film. Therefore, the thermal diffusivity of DDSQ-grafted PSQ films prepared in the study with different amounts of DDSQ was measured and compared with that of hybrid films containing POSS molecules.

The thermal diffusivities of DDSQ-grafted PSQ films containing 5–25 mol% vinyl-DDSQ are shown in Figure 4.5 and Table 4.1, along with those of an MSQ film prepared via the dehydrogenation reaction of MSQ-SiH and POSS-containing hybrid films prepared via hydrosilylation [44]. As we previously reported, the MSQ film exhibits a high thermal diffusivity of 1.44×10^{-7} m^2/s due to the formation of a highly cross-linked network structure. Interestingly, the thermal diffusivity of the DDSQ-grafted PSQ film containing 5 mol% DDSQ decreased to 1.21×10^{-7} m^2/s, and further decreased to 1.02×10^{-7} m^2/s proportionally with increasing the DDSQ amounts in the range of 5–25 mol% (Figure 4.5 and Table 4.1). The introduction of the DDSQ structure apparently enhances the thermal insulating properties similarly to that observed for the POSS-containing hybrid films, although the latter exhibited lower thermal diffusivity than the former, as shown in Figure 4.5 and Table 4.1. These results indicate that intramolecular void spaces were formed around the DDSQ structure because of the formation of $Si–CH_2CH_2–Si$ bonds.

The influence of the amount of Pt catalyst on the thermal diffusivity of the DDSQ-grafted PSQ films was also investigated. In this experiment, the same Pt catalyst amount as used in the hydrosilylation reaction was added to DDSQ-grafted PSQ, and the dehydrogenation reaction was conducted. Light-brown DDSQ-grafted PSQ films containing 5–25 mol% DDSQ were obtained.

Although the thermal diffusivities of these films also decreased with increasing amounts of DDSQ (Figure 4.6), considerable differences in the values were observed, most likely because the additional Pt catalyst increased the reaction rate of the dehydrogenation, which became uncontrolled.

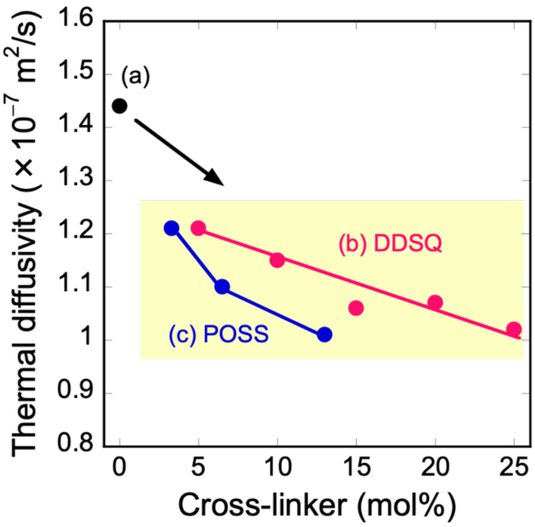

Figure 4.5 Thermal diffusivities of (a) an MSQ film (black circle), (b) DDSQ-grafted PSQ films prepared via the hydrosilylation reaction between MSQ-SiH and vinyl-DDSQ (pink circles), and (c) POSS-containing PSQ films prepared via the hydrosilylation reaction between MSQ-SiH and vinyl-POSS (blue circles).

Table 4.1. Thermal diffusivities of an MSQ film, DDSQ-grafted PSQ films, and POSS-containing hybrid films

oligosilsesquioxane	Vinyl-DDSQ (mol%)	Vinyl-POSS (wt%)[a]	thermal diffusivity[b] (m^2/s)
MSQ-SiH	0		1.44×10^{-7}[c]
MSQ-SiH	5		1.21×10^{-7}
MSQ-SiH	10		1.15×10^{-7}
MSQ-SiH	15		1.06×10^{-7}
MSQ-SiH	20		1.07×10^{-7}
MSQ-SiH	25		1.02×10^{-7}
MSQ-SiH		5 (3.3 mol%)	1.21×10^{-7}
MSQ-SiH		10 (6.5 mol%)	1.10×10^{-7}
MSQ-SiH		20 (13 mol%)	1.01×10^{-7}

[a] The data were obtained from ref. [43].

[b] The measurements were repeated nine times, and the average value was calculated.

[c] The data were obtained from ref. [44].

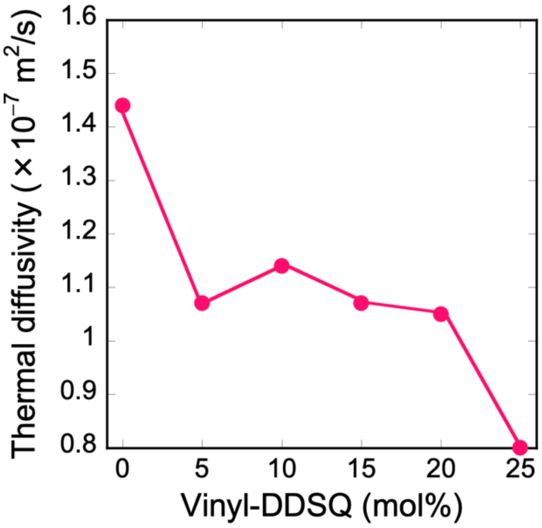

Figure 4.6 Thermal diffusivities of DDSQ-grafted PSQ films prepared by adding Platinum catalyst before the dehydrogenation reaction.

To gain insight into the formation of intramolecular void spaces around the DDSQ molecules in the PSQ film, the lifetime spectra of positron annihilation were measured for DDSQ-grafted PSQ films containing 10 and 20 mol% DDSQ. The probability density function (PDF) of the annihilation rate was obtained using a numerical Laplace inversion technique (Figure 4.7). The spectra were decomposed into four components, and the lifetime corresponding to the pick-off annihilation of *ortho*-positronium (τ_{ps}) and the corresponding intensity (I_{Ps}) were derived. Table 4.2 summarizes the obtained parameters and the values of free volume (V) estimated using τ_{ps} according to the Tao–Eldrup model [46, 47]. Compared with a DDSQ-free MSQ film, the DDSQ-grafted PSQ film containing 10 mol% DDSQ exhibited a slightly higher τ_{ps} value of 0.35 ns, which is consistent with the formation of void spaces in the ethylene-bridged structure producing a subtle increase in the lifetime. The V value for the DDSQ-grafted PSQ film containing 10 mol% DDSQ was 0.24 nm^3, which was larger than that of the MSQ film (0.23 nm^3) [44]. However, the V value for the DDSQ-grafted PSQ film containing 20 mol% DDSQ was estimated to be 0.22 nm^3, which was smaller than that of the MSQ film and the DDSQ-grafted PSQ film containing 10 mol% DDSQ. Moreover, the peak top of PDF for the DDSQ-grafted PSQ film containing 20 mol% DDSQ shifts slightly to a shorter time region (Figure 4.7), and a clear difference in the V value was not observed. These results suggest that the decrease in the thermal diffusivity might not stem from the intramolecular void spaces formed by the hydrosilylation reaction.

The highly cross-linked network of the MSQ film provided a heat conduction pathway that enhanced the thermal diffusivity. In contrast, since vinyl-DDSQ has only two vinyl groups for the hydrosilylation reaction, the crosslinking degree should be lower in the DDSQ-grafted PSQ films containing 10 mol% and 20 mol% DDSQ. This would be detrimental to heat conduction pathways, resulting in lower thermal diffusivity than that of the MSQ film. Meanwhile, although the POSS-containing hybrid films exhibited highly cross-linked networks because of the eight vinyl groups, the decrease in the thermal diffusivity can be attributed to the formation of intramolecular void spaces because the rigidity of the hybrid films would prevent collapse of the void spaces. In the case of the DDSQ-grafted PSQ films, the hardness of the DDSQ-grafted PSQ films decreased with increasing the vinyl-DDSQ content from 5 to 25 mol%, namely, the crosslinking density decreased, which could disrupt the intramolecular void spaces, especially for the DDSQ-grafted PSQ film containing 25 mol% DDSQ. Therefore, the decrease in the thermal diffusivity of the DDSQ-grafted PSQ films could be due to a decrease in the crosslinking density. To gain the information about the cross-linking density, the storage modulus (E′) and the loss modulus (E″) of DDSQ-grafted PSQ film containing 10 mol% DDSQ molecules were measured between −150 to 250 °C by a heating rate of 5 °C/min at a frequency of 10 kHz (Figure 4.8). In the DDSQ-grafted PSQ film containing 10 mol% DDSQ molecules, the distinct peaks were observed in the E″ in the glass-relaxation region. DDSQ-grafted PSQ film apparently exhibited rubber-like property. The cross-linking density of DDSQ-grafted PSQ film containing 10 mol% DDSQ molecules could be estimated to be 7.27 × 10^{-4} mol/cm^3 by the following equation (4.1):

$$crosslinking\ density\ = {}^{E'}/_{3 \cdot R \cdot T} \tag{4.1}$$

where E' is the storage modulus at 150 °C. R and T are the gas constant and absolute temperature, respectively. The further studies are underway to clarify the effect of DDSQ molecules in PSQ network on the relationship between the crosslinking density and the mechanical and thermal insulating property.

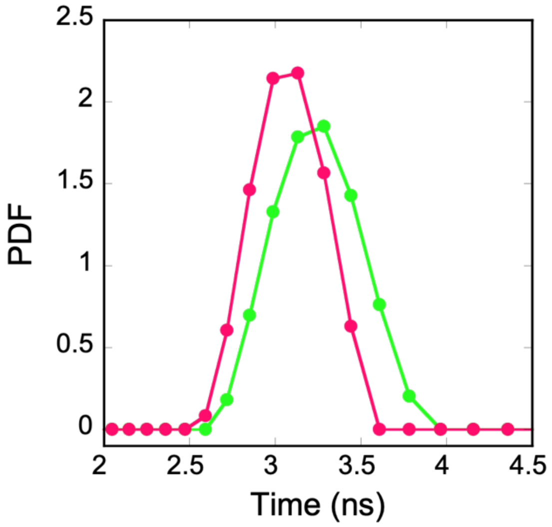

Figure 4.7 PDF of the lifetime of *ortho*-positronium in DDSQ-grated PSQ films prepared from MSQ-SiH and 5 mol % (pink circles) and 10 mol% (green circles) of vinyl-DDSQ by the hydrosilylation reaction.

Table 4.2. Lifetime (τ_{ps}), relative intensity (I_{ps}), and free volume (V) for the annihilation of *ortho*-positronium in an MSQ film prepared via hydrogenation of MSQ-SiH and DDSQ-grafted PSQ films prepared by the hydrosilylation reaction between MSQ-SiH and 5 and 10 mol% vinyl-DDSQ

silsesquioxane	Vinyl-DDSQ (mol%)	τ_{pso} (ns)[b]	I_{ps} (%)[b]	V (nm^3)[a,b]
MSQ-SiH	0	3.29 ± 0.01[c]	38[c]	0.23[c]
MSQ-SiH	10	3.35 ± 0.01	35	0.24
MSQ-SiH	20	3.20 ± 0.01	36	0.22

[a]The values of free volume were estimated using the Tao–Eldrup equation ref. [46, 47]. [b]Lifetime (τ_{ps}), relative intensity (I_{ps}), and free volume (V).

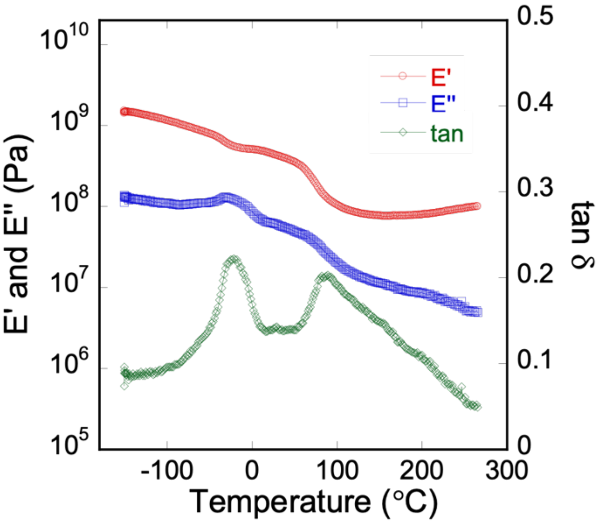

Figure 4.8 Temperature dependence of the storage modulus (E′), loss modulus (E″), and loss tangent (tan δ) for DDSQ-grafted PSQ film containing 10 mol% DDSQ molecules.

4.2.3 Thermal stability of the DDSQ-grafted PSQ films

As mentioned in the Introduction, high thermal stability is required for next-generation thermal insulation materials. We previously reported that an MSQ film prepared via dehydrogenation of the hydrosilyl groups exhibited high thermal stability over 450 °C.[25] In this study, the influence of the DDSQ structure having a rigid core composed of siloxane bonds on the thermal stability of the DDSQ-grafted PSQ films was investigated by performing a thermogravimetry/differential thermal analysis (TG/DTA), and the results are summarized in Figure 4.9 and Table 4.3.

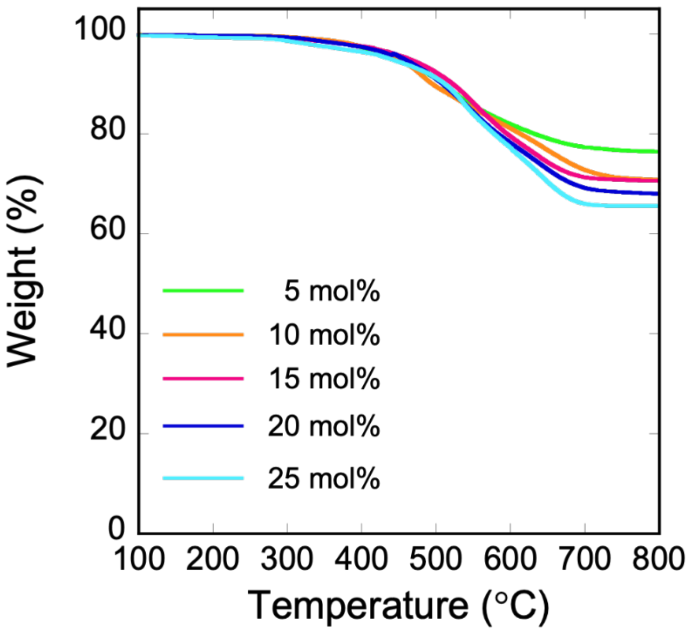

Figure 4.9 Thermogravimetric analysis traces of DDSQ-grafted PSQ films containing DDSQ molecules (5–25 mol%) measured at a heating rate of 10 °C/min under an air flow of 100 mL/min.

Compared with an ethylene-bridged PSQ film prepared via the hydrosilylation reaction of MSQ-SiH with MSQ-SiVi, which exhibited a 5% mass loss temperature (T_d^5) of 302 °C and a 10% weight loss temperature (T_d^{10}) of 285 °C [43], the DDSQ-grafted PSQ films showed higher thermal stability, with T_d^5 and T_d^{10} values of 438 °C–463 °C and 495 °C–523 °C, respectively (Table 4.3). This result is in agreement with previous studies on polyurethane, polysiloxane, and polyimide containing DDSQ in the main chain, which exhibited enhanced thermal stability with a T_d^5 of 300 °C–550 °C compared with the corresponding DDSQ-free polymers due to the rigid structure of DDSQ [64-66], and confirms the enhancing effect of DDSQ in the thermal stability of the DDSQ-grafted PSQ films. Differential scanning calorimetry (DSC) of DDSQ-grafted PSQ films containing 5–25 mol% DDSQ was also performed as additional information regarding the thermal property. The endothermic peaks or glass transition temperature like peaks were observed at around 42 °C not depending on the amount of DDSQ molecules (Figure 4.10). The origin of these peaks was unclear, but it might be derived from the nature of PSQ network.

As shown in Table 4.3, although POSS-containing hybrid films also exhibited high thermal stability compared with the organic polymer [44], their T_d^5 and T_d^{10} values decreased with an increase in the amount of POSS because the remaining vinyl group and the formed Si–CH_2CH_2–Si bonds, which are less thermally stable than Si–O–Si bonds, reduce the thermal stability of the hybrid films. However, the vinyl group was completely consumed in the two-step reaction leading to DDSQ-grafted PSQ films, resulting in higher thermal stability. To prevent the side reaction during the preparation of the POSS-containing films, a similar two-step reaction was conducted to obtain a hybrid film containing 10 wt% POSS.

A ^{1}H NMR analysis revealed that the vinyl group of vinyl-POSS completely disappeared after conducting the hydrosilylation reaction of MSQ-SiH and vinyl-POSS overnight. The obtained freestanding film containing 10 wt% POSS was colorless after the dehydrogenation reaction; however, for unknown reasons, the surface was considerably rough even though the aggregation of POSS molecules was prevented. In addition, the T_d^5 and T_d^{10} of the hybrid film containing 10 wt% POSS were 360 °C and 422 °C, respectively. Overall, the two-step reaction did not improve the thermal stability of hybrid films containing POSS. Since the vinyl group disappeared after the hydrosilylation reaction, the lower thermal stability of the POSS-containing hybrid film could be attributed to the unstable Si–CH_2CH_2–Si bonds. Furthermore, the DDSQ-grafted PSQ films showed excellent thermal stability compared with an MSQ/TAIC hybrid film, in which the TAIC molecules decreased the thermal diffusivity but the thermal stability was reduced with increasing the amount of TAIC; an MSQ/TAIC film with a hydrosilyl group/allyl group molar ratio of 1/1 exhibited a T_d^5 of 380 °C and a T_d^{10} of 427 °C (Chapter 3). In the DDSQ-grafted PSQ films, the thermal diffusivity decreased upon incorporating the DDSQ structure in the siloxane network, while a high thermal stability over 400 °C was maintained.

Table 4.3. Thermal stability of an ethylene-bridged PSQ film, DDSQ-grafted PSQ films, and POSS-containing hybrid films[a]

oligosilsesquioxane	Vinyl-DDSQ (mol%)	Vinyl-POSS (wt%)[a]	T_d^5 (%)	T_d^{10} (%)
MSQ-SiH/MSQ-SiVi	0		302[b]	285[b]
MSQ-SiH	5		445	510
MSQ-SiH	10		448	495
MSQ-SiH	15		463	523
MSQ-SiH	20		456	509
MSQ-SiH	25		438	512
MSQ-SiH		5 (3.3 mol%)	382[b]	453[b]
MSQ-SiH		10 (6.5 mol%)	370[b]	448[b]
MSQ-SiH		20 (13 mol%)	304[b]	397[b]

[a] Measured at a heating rate of 10 °C under an air flow of 50–100 mL/min.

[b] The data were obtained from ref. [43, 44].

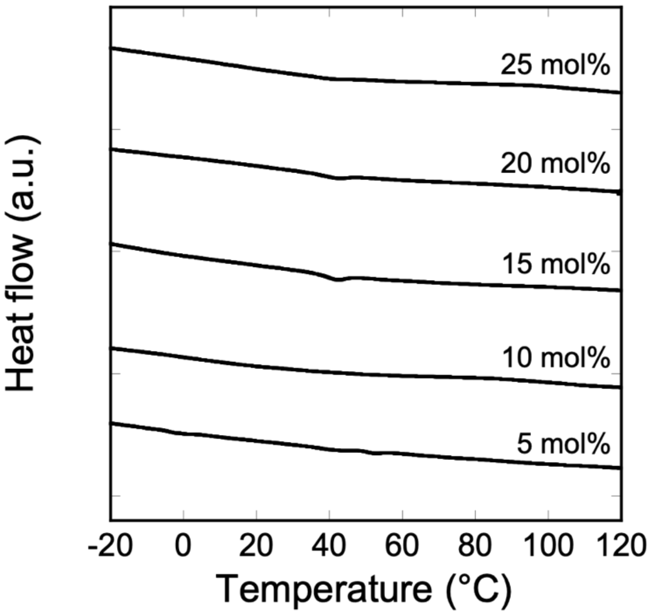

Figure 4.10 DSC curves of DDSQ-grafted PSQ films containing 5–25 mol% of DDSQ.

4.3 Conclusions

DDSQ-grafted PSQ films containing 5–25 mol% of DDSQ were prepared following a two-step process. First, the hydrosilylation reaction between MSQ-SiH and vinyl-DDSQ forming Si–CH_2CH_2–Si bonds was conducted in solution under a nitrogen atmosphere to prevent the dehydrogenation side reaction induced by moisture, and the successive dehydrogenation reaction of the remaining SiH groups was then conducted in the film state to promote the crosslinking reaction via the formation of Si–O–Si bonds. By conducting the two-step reaction, the dehydrogenation reaction of the SiH groups during the hydrosilylation reaction in solution was prevented and the Si–CH_2CH_2–Si bonds were formed quantitatively, according to ^{1}H NMR and FT-IR analyses.

Unlike POSS-containing hybrid films, the high miscibility of the DDSQ molecule allowed introducing a high amount of vinyl-DDSQ as a crosslinker, obtaining colorless and transparent DDSQ-grafted PSQ films without aggregation of the DDSQ molecules. The thermal diffusivities of the DDSQ-grafted PSQ films decreased from 1.21×10^{-7} to 1.02×10^{-7} m^2/s with increasing the DDSQ amount from 5 to 25 mol%, as was similarly observed for POSS-containing hybrid films. However, the hardness of the DDSQ-grafted PSQ films decreased with an increase in the vinyl-DDSQ content. The V value for DDSQ-grafted PSQ films containing 5 and 10 mol% DDSQ estimated from a positron annihilation lifetime analysis was 0.24 and 0.22 nm^3, respectively, and a clear relationship between the thermal diffusivity and the volume size was not observed. These results indicate that the low thermal diffusivity of the DDSQ-grafted PSQ films did not stem from the formation of intramolecular void spaces but from a decrease in the crosslinking density upon the introduction of the DDSQ structure. The DDSQ-grafted PSQ films maintained high thermal stability over 400 °C with T_d^5 and T_d^{10} values of 438 °C–463 °C and 495 °C–523 °C, respectively, outperforming POSS-containing hybrid films. According to their high thermal insulating properties and thermal stability, the DDSQ-grafted PSQ films can be considered promising materials for next-generation thermal insulators.

4.4 Experimental

Materials

MSQ-SiH was prepared according to our previous paper.[19] Vinyl-DDSQ was provided by JNC Corporation and used as received. THF (super dehydrated) and toluene (super dehydrated) were purchased from FUJIFILM Wako Pure Chemical Co., Ltd. Platinum(0)-1,3-divinyl-1,1,3,3-tetramethyldisiloxane complex solution (Karstedt's catalyst) in xylene was purchased from Sigma-Aldrich.

Characterization

^{1}H NMR measurements were performed on a Varian 400 MHz spectrometer, and ^{29}Si NMR measurement was performed on a Varian 500 MHz spectrometer. GPC was performed on a Shimadzu LC-20AD HPLC systems using triply connected TSKgel SW columns. THF was used as the eluent at a flow rate of 1 mL/min and the molecular weight was calibrated using polystyrene standards. ATR-FT-IR spectra were recorded on a Shimadzu IR Affinity-1 spectrometer equipped with an ATR unit. TG/DTA was performed on an SII EXSTAR TG-DTA 6200 thermal analyzer at a heating rate of 10 °C/min under an air flow of 50 mL/min. DSC was performed on HITACHI DSC7000X thermal analyzer at a heating rate of 10 °C/min under a nitrogen. AFM measurement was conducted using AFM-5500M HITACHI microscope. Thermal diffusivity measurements were performed on an ai-phase Mobile M3 type 1 system. The measurements were repeated nine times and the averaged thermal diffusivity was calculated. Positron lifetime measurements were performed using a system based on a digital oscilloscope. The detailed procedure was described in our previous paper.[20] Dynamic mechanical analysis was performed on Hitachi HighTech DMA6110. The measurements of specimens with width of 9.1 mm and thickness of 0.4 mm were conducted from −150 to 250 °C at a heating rate of 5 °C/min and a frequency of 10 Hz.

Preparation of DDSQ-grafted PSQ films via the hydrosilylation reaction of MSQ-SiH with vinyl-DDSQ and successive dehydrogenation reaction

A typical preparation procedure was as follows: In a 25 mL flask, MSQ-SiH (0.500 g, 1.21 mmol) and vinyl-DDSQ (0.219 g, 0.182 mmol) were dissolved in 5- mL THF and stirred at room temperature for 10 min under a nitrogen atmosphere. Then, 5 wt% Karstedt's catalyst solution in THF (0.0250 g) was added and stirred at 50 °C overnight. The solvent was removed using an evaporator, affording a colorless and viscous liquid. Then, the hybrid films were prepared according to the following procedure: A portion of the viscous liquid was added to a PFA vial with an inner diameter of 18.4 mm and heated in an oven under air atmosphere at 80, 100, 120, and 140 °C for 1 h at each temperature and at 160 °C for 4 h to obtain freestanding gel films. For the experiment of the dehydrogenation reaction with an additional amount of Karstedt's catalyst, a half amount of the polymer obtained after the hydrosilylation and 0.0125 g of 5 wt% Karstedt's catalyst solution in toluene were stirred for 10 min. Then, the mixture was transferred to a PFA vial with an inner diameter of 18.4 mm and heated in an oven under air atmosphere at the same conditions described above for the DDSQ-grafted PSQ films.

Chapter 5 Conclusions

In conclusion, the relationship between structure and thermal properties is investigated for the creation of new PSQ-based insulating materials. Furthermore, we proposed a strategy to introduce crosslinkers into PSQs to improve their adiabatic properties and thermal stability.

In Chapter 2, a series of PSQs were prepared by sol-gel reaction and the effects of residual alkoxy groups and substituents on the thermal insulating properties of the corresponding freestanding gel films were investigated. The thermal diffusivity of freestanding gel films prepared from PSQ-Me (OEt) and PSQ-Me (OBu^i) was found to decrease as the amount of residual alkoxy groups decreased. The substituents on the silicon atoms also affected the thermal insulator properties. The thermal stability of PSQ-Ph films was considerably higher than that of PSQ-Me and PSQ-Phe films. However, despite the presence of a phenyl ring in PSQ-Phe, its thermal stability was lower than that of PSQ-Me and PSQ-Ph, possibly due to the instability of the benzyl group at high temperatures in air.

In Chapter 3, MSQ/TAIC hybrid films with isocyanurate rings were prepared by hybridizing MSQ and TAIC by hydrosilylation. TAIC exhibited excellent solubility and miscibility as a cross-linker. The adiabatic performance of the MSQ/TAIC hybrid film was improved with increasing TAIC content, and was higher than that of the TAIC-free MSQ film prepared by MSQ-SiH coupling reaction and the PSQ/TESIC film prepared by polycondensation of the ethoxysilane precursors. Positron annihilation lifetime analysis revealed that the improved adiabatic performance is not due to the formation of intramolecular voids but to the nature of the isocyanurate ring.

In Chapter 4, a homogeneous PSQ gel film without aggregation was successfully prepared by performing a hydrosilylation reaction between MSQ-SiH and vinyl-DDSQ with phenyl groups on silicon atoms, followed by successive dehydrogenation reactions of the remaining SiH groups in the film state with moisture. It was found that the adiabatic performance was improved when the DDSQ content was increased from 5 to 25 mol%. The DDSQ-containing PSQ films showed lower thermal diffusivity than those prepared from similar reactions of vinyl-POSS reported previously, which was not due to the formation of intramolecular voids but to the reduction of crosslink density associated with the introduction of DDSQ structure. Furthermore, the DDSQ-grafted PSQ films maintained excellent thermal stability above 400 °C.

In summary, a variety of PSQ-based hybrid gel films were prepared and their adiabatic performance was significantly improved by tuning the PSQ chemical structure during the course of the studies. These findings are expected to lead to the development of next-generation insulation materials with higher performance.

List of publications

Chapter 2. Structure–Thermal Property Relationships of Polysilsesquioxanes for Thermal Insulation Materials
Takashi Hamada, Taku Goto, Sakino Takase, Kenta Okada, Akira Uedono, and Joji Ohshita
ACS Applied Polymer Materials **2022**, *4*, 4, 2851-2859.

Chapter 3. Organic–Inorganic Hybrid Thermal Insulation Materials Prepared via Hydrosilylation of Polysilsesquioxane Having Hydrosilyl Groups and Triallylisocyanurate
Sakino Takase, Takashi Hamada, Kenta Okada, Susumu Mineoi, Akira Uedono, and Joji Ohshita
ACS Applied Polymer Materials **2022**, *4*, 5, 3726–3733.

Chapter 4. Double-Decker Silsesquioxane-Grafted Polysilsesquioxane Hybrid Films as Thermal Insulation Materials
Takashi Hamada, Sakino Takase, Arata Tanaka, Kenta Okada, Susumu Mineoi, Akira Uedono, and Joji Ohshita
ACS Applied Polymer Materials **2023**, *5*, 1, 743–750.

This dissertation includes contents reproduced from the papers listed above with permission. Copyright 2022 ACS.

Other papers not included in this thesis

Polysilsesquioxane-Containing Thermally Degradable Groups for Potential Application as Thermal Insulation Materials
Sakino Takase, Takashi Hamada, Kenta Okada, Susumu Mineoi, and Joji Ohshita
ACS Applied Polymer Materials **2023**, *5*, 2, 1390–1397.

Bibliography

[1] R. Hannah, R. Max, R. Pablo, CO_2 and Greenhouse Gas Emissions, Published online at OurWorldInData.org. 2020.

[2] S.S. Chandel, R. Shrivastva, V. Sharma, P. Ramasamy, Overview of the initiatives in renewable energy sector under the national action plan on climate change in India, Renewable & Sustainable Energy Reviews 54 (2016) 866-873.

[3] P.M. Cox, R.A. Betts, C.D. Jones, S.A. Spall, I.J. Totterdell, Acceleration of global warming due to carbon-cycle feedbacks in a coupled climate model, Nature 408(6809) (2000) 184-187.

[4] S.C. Pereira, D. Carvalho, A. Rocha, Temperature and Precipitation Extremes over the Iberian Peninsula under Climate Change Scenarios: A Review, Climate 9(9) (2021).

[5] F. Sher, D. Raore, J.J. Klemes, P.M. Rafi-ul-Shan, M. Khzouz, K. Marintseva, O. Razmkhah, Unprecedented Impacts of Aviation Emissions on Global Environmental and Climate Change Scenario, Current Pollution Reports 7(4) (2021) 549-564.

[6] R.N.E. Huaman, T.X. Jun, Energy related CO2 emissions and the progress on CCS projects: A review, Renewable & Sustainable Energy Reviews 31 (2014) 368-385.

[7] P. Friedlingstein *et al.*, Global Carbon Budget 2022, Earth Syst. Sci. Data, 2022, pp. 4811–4900.

[8] P.L. Hurtado, A. Rouilly, V. Vandenbossche, C. Raynaud, A review on the properties of cellulose fibre insulation, Building and Environment 96 (2016) 170-177.

[9] M.S. Al-Homoud, Performance characteristics and practical applications of common building thermal insulation materials, Building and Environment 40(3) (2005) 353-366.

[10] H. Zhang, W.Z. Fang, Y.M. Li, W.Q. Tao, Experimental study of the thermal conductivity of polyurethane foams, Applied Thermal Engineering 115 (2017) 528-538.

[11] L.D. Hung, Z. Pasztory, An overview of factors influencing thermal conductivity of building insulation materials, Journal of Building Engineering 44 (2021).

[12] A.M. Papadopoulos, State of the art in thermal insulation materials and aims for future developments, Energy and Buildings 37(1) (2005) 77-86.

[13] E. Cuce, P.M. Cuce, C.J. Wood, S.B. Riffat, Toward aerogel based thermal superinsulation in buildings: A comprehensive review, Renewable & Sustainable Energy Reviews 34 (2014) 273-299.

[14] S. Schiavoni, F. D'Alessandro, F. Bianchi, F. Asdrubali, Insulation materials for the building sector: A review and comparative analysis, Renewable & Sustainable Energy Reviews 62 (2016) 988-1011.

[15] D.K. Chattopadhyay, D.C. Webster, Thermal stability and flame retardancy of polyurethanes, Progress in Polymer Science 34(10) (2009) 1068-1133.

[16] S.T. McKenna, T.R. Hull, The fire toxicity of polyurethane foams, Fire Sci. Rev., 2016.

[17] D. Allan, J. Daly, J.J. Liggat, Thermal volatilisation analysis of TDI-based flexible polyurethane foam, Polymer Degradation and Stability 98(2) (2013) 535-541.

[18] Y. Yuan, W. Wang, Y.Q. Shi, L. Song, C. Ma, Y. Hu, The influence of highly dispersed Cu2O-anchored MoS2 hybrids on reducing smoke toxicity and fire hazards for rigid polyurethane foam, Journal of Hazardous Materials 382 (2020).

[19] F. Bjork, T. Enochsson, Properties of thermal insulation materials during extreme environment changes, Construction and Building Materials 23(6) (2009) 2189-2195.

[20] H.H. Liao, H.Y. Li, Y. Liu, Q. Wang, A flame-retardant composite foam: foaming polyurethane in melamine formaldehyde foam skeleton, Polymer International 68(3) (2019) 410-417.

[21] C.P. Ruan, K.L. Ai, X.B. Li, L.H. Lu, A Superhydrophobic Sponge with Excellent Absorbency and Flame Retardancy, Angewandte Chemie-International Edition 53(22) (2014) 5556-5560.

[22] R.K. Chinnam, A.A. Francis, J. Will, E. Bernardo, A.R. Boccaccini, Review. Functional glasses and glass-ceramics derived from iron rich waste and combination of industrial residues, Journal of Non-Crystalline Solids 365 (2013) 63-74.

[23] D.I. Saparuddin, N.A.N. Hisham, S.A. Ab Aziz, K.A. Matori, S. Honda, Y. Iwamoto, M.H.M. Zaid, Effect of sintering temperature on the crystal growth, microstructure and mechanical strength of foam glass-ceramic from waste materials, Journal of Materials Research and Technology-Jmr&T 9(3) (2020) 5640-5647.

[24] A. Siddika, A. Hajimohammadi, V. Sahajwalla, Powder sintering and gel casting methods in making glass foam using waste glass: A review on parameters, performance, and challenges, Ceramics International 48(2) (2022) 1494-1511.

[25] X.Y. Liu, Y.X. Wu, X.C. Zhao, Z.K. Wang, Fabrication and applications of bioactive chitosan-based organic-inorganic hybrid materials: A review, Carbohydrate Polymers 267 (2021).

[26] Z.H. Huang, K.Y. Qiu, PREPARATION AND THERMAL-PROPERTY OF POLY(METHYL METHACRYLATE)/SILICATE HYBRID MATERIALS BY THE IN-SITU SOL-GEL PROCESS, Polymer Bulletin 35(5) (1995) 607-613.

[27] H.T. Wang, P. Xu, W. Zhong, L. Shen, Q.G. Du, Transparent poly(methyl methacrylate)/silica/zirconia nanocomposites with excellent thermal stabilities, Polymer Degradation and Stability 87(2) (2005) 319-327.

[28] S. Hamdani, C. Longuet, D. Perrin, J.M. Lopez-Cuesta, F. Ganachaud, Flame retardancy of silicone-based materials, Polymer Degradation and Stability 94(4) (2009) 465-495.

[29] J. Kozakiewicz, I. Ofat, J. Trzaskowska, Silicone-containing aqueous polymer dispersions with hybrid particle structure, Advances in Colloid and Interface Science 223 (2015) 1-39.

[30] R. Oban, K. Matsukawa, A. Matsumoto, Heat resistant and transparent organic-inorganic hybrid materials composed of N-allylmaleimide copolymer and random-type SH-modified silsesquioxane, Journal of Polymer Science Part a-Polymer Chemistry 56(20) (2018) 2294-2302.

[31] T. Maeda, T. Hamada, S. Tsukada, D. Katsura, K. Okada, J. Ohshita, Antifogging Hybrid Materials Based on Amino-Functionalized Polysilsesquioxanes, Acs Applied Polymer Materials 3(5) (2021) 2568-2575.

[32] D. Zhang, M. Kanezashi, T. Tsuru, K. Yamamoto, T. Gunji, Y. Adachi, J. Ohshita, Development of PSQ-RO membranes with high water permeability by copolymerization of bis 3-(triethoxysilyl)propyl amine and triethoxy (3-glycidyloxypropyl)silane, Journal of Membrane Science 644 (2022).

[33] D. Zhang, M. Kanezashi, T. Tsuru, K. Yamamoto, R. Yakuwa, T. Gunji, Y. Adachi, J. Ohshita, Preparation of polysilsesquioxane reverse osmosis membranes for water desalination from tris (ethoxysilyl)alkyl amines by sol-gel process and interfacial polymerization, Applied Organometallic Chemistry 35(11) (2021).

[34] J. Ohshita, T. Okonogi, K. Kajimura, K. Horata, Y. Adachi, M. Kanezashi, T. Tsuru, Preparation of amine- and ammonium-containing polysilsesquioxane membranes for CO2 separation, Polymer Journal 54(7) (2022) 875-882.

[35] W.C. Chen, L.H. Lee, B.F. Chen, C.T. Yen, Synthesis and characterization of poly(methyl silsesquioxane)titania optical thin films, Journal of Materials Chemistry 12(12) (2002) 3644-3648.

[36] L.H. Lee, W.C. Chen, W.C. Liu, Structural control of oligomeric methyl silsesquioxane precursors and their thin-film properties, Journal of Polymer Science Part a-Polymer Chemistry 40(10) (2002) 1560-1571.

[37] Z.N. Bao, V. Kuck, J.A. Rogers, M.A. Paczkowski, Silsesquioxane resins as high-performance solution processible dielectric materials for organic transistor applications, Advanced Functional Materials 12(8) (2002) 526-531.

[38] A. Harada, K. Shikinaka, J. Ohshita, Y. Kaneko, Preparation of a one-dimensional soluble polysilsesquioxane containing phosphonic acid side-chain groups and its thermal and proton-conduction properties, Polymer 121 (2017) 228-233.

[39] Y. Kaneko, Ionic silsesquioxanes: Preparation, structure control, characterization, and applications, Polymer 144 (2018) 205-224.

[40] H. Zhou, Q. Ye, J.W. Xu, Polyhedral oligomeric silsesquioxane-based hybrid materials and their applications, Materials Chemistry Frontiers 1(2) (2017) 212-230.

[41] N. Ahmed, H. Fan, P. Dubois, X.W. Zhang, S. Fahad, T. Aziz, J.T. Wan, Nano-engineering and micromolecular science of polysilsesquioxane materials and their emerging applications, Journal of Materials Chemistry A 7(38) (2019) 21577-21604.

[42] A.V. Rao, S.D. Bhagat, H. Hirashima, G.M. Pajonk, Synthesis of flexible silica aerogels using methyltrimethoxysilane (MTMS) precursor, Journal of Colloid and Interface Science 300(1) (2006) 279-285.

[43] T. Hamada, Y. Nakanishi, K. Okada, J. Ohshita, Crack- and Shrinkage-Free Ethylene-Bridged Polysilsesquioxane Film Prepared by a Hydrosilylation Reaction, Acs Omega 6(12) (2021) 8430-8437.

[44] T. Hamada, Y. Nakanishi, K. Okada, S. Tsukada, A. Uedono, J. Ohshita, Thermal Insulating Property of Silsesquioxane Hybrid Film Induced by Intramolecular Void Spaces, Acs Applied Polymer Materials 3(7) (2021) 3383-3391.

[45] T. Gunji, Y. Iizuka, K. Arimitsu, Y. Abe, Preparation and properties of alkoxy(methyl)silsesquioxanes as coating agents, Journal of Polymer Science Part a-Polymer Chemistry 42(15) (2004) 3676-3684.

[46] S.J. Tao, POSITRONIUM ANNIHILATION IN MOLECULAR SUBSTANCES, Journal of Chemical Physics 56(11) (1972) 5499-5510.

[47] M. Eldrup, D. Lightbody, J.N. Sherwood, THE TEMPERATURE-DEPENDENCE OF POSITRON LIFETIMES IN SOLID PIVALIC ACID, Chemical Physics 63(1-2) (1981) 51-58.

[48] M. Hashimoto, H. Imoto, K. Matsukawa, K. Naka, Coexistence of Optical Transparency, Hydrophobicity, and High Thermal Conductivity in Beads-on-String-Shaped Polyureas Induced by Disordered Hydrogen-Bond Networks, Macromolecules 53(8) (2020) 2874-2881.

[49] R.H. Baney, M. Itoh, A. Sakakibara, T. Suzuki, SILSESQUIOXANES, Chemical Reviews 95(5) (1995) 1409-1430.

[50] X.Q. Xu, C.A. Wu, B.H. Zhang, H. Dong, Preparation, structure characterization, and thermal performance of phenyl-modified MQ silicone resins, Journal of Applied Polymer Science 128(6) (2013) 4189-4200.

[51] S. Pohl, O. Janka, E. Fuglein, G. Kickelbick, Thermoplastic Silsesquioxane Hybrid Polymers with a Local Ladder-Type Structure, Macromolecules 54(8) (2021) 3873-3885.

[52] G.G. Cameron, D.R. Kane, THERMAL DEGRADATION OF POLY(BENZYL ACRYLATE), Polymer 9(9) (1968) 461-470.

[53] A. Jitianu, G. Amatucci, L.C. Klein, Phenyl-Substituted Siloxane Hybrid Gels that Soften Below 140 degrees C, Journal of the American Ceramic Society 92(1) (2009) 36-40.

[54] N. Steinbruck, S. Pohl, G. Kickelbick, Platinum free thermally curable siloxanes for optoelectronic application - synthesis and properties, Rsc Advances 9(4) (2019) 2205-2216.

[55] M. Moritsugu, A. Sudo, T. Endo, Cyclotrimerization of diisocyanates toward high-performance networked polymers with rigid isocyanurate structure: Combination of aromatic and aliphatic diisocyanates for tunable flexibility, Journal of Polymer Science Part a-Polymer Chemistry 51(12) (2013) 2631-2637.

[56] M. Moritsugu, A. Sudo, T. Endo, Development of High-Performance Networked Polymers Consisting of Isocyanurate Structures Based on Selective Cyclotrimerization of Isocyanates, Journal of Polymer Science Part a-Polymer Chemistry 49(24) (2011) 5186-5191.

[57] S. Okamoto, T. Endo, Synthesis and radical polymerization of acrylate and methacrylate bearing an isocyanurate core with adamantyl bisurethane moieties, Journal of Polymer Science 59(24) (2021) 3141-3149.

[58] X.L. Huang, J. Guo, Y.M. Gong, S.L. Li, S.Y. Mu, S. Zhang, In-situ preparation of a shape stable phase change material, Renewable Energy 108 (2017) 244-249.

[59] R.B. Gregory, ANALYSIS OF POSITRON-ANNIHILATION LIFETIME DATA BY NUMERICAL LAPLACE INVERSION - CORRECTIONS FOR SOURCE TERMS AND ZERO-TIME SHIFT ERRORS, Nuclear Instruments & Methods in Physics Research Section a-Accelerators Spectrometers Detectors and Associated Equipment 302(3) (1991) 496-507.

[60] A.R. Jennings, A.M. Morey, A.J. Guenthner, S.T. Iacono, Synthesis and characterization of siloxane-based cyanate ester elastomers from readily availablematerials: a top-down approach, Polymer International 66(4) (2017) 540-547.

[61] C.D. Li, Z.F. Chen, W.F. Dong, L.L. Lin, X.M. Zhu, Q.S. Liu, Y. Zhang, N. Zhai, Z.H. Zhou, Y.H. Wang, B.M. Chen, Y.X. Ji, X.Q. Chen, X.C. Xu, Y.F. Yang, H.T. Zhang, A review of

silicon-based aerogel thermal insulation materials: Performance optimization through composition and microstructure, Journal of Non-Crystalline Solids 553 (2021).

[62] M. Seino, T. Hayakawa, Y. Ishida, M. Kakimoto, K. Watanabe, H. Oikawa, Hydrosilylation polymerization of double-decker-shaped silsesquioxane having hydrosilane with diynes, Macromolecules 39(10) (2006) 3473-3475.

[63] K. Yoshida, K. Ito, H. Oikawa, M. Yamahiro, Y. Morimoto, K. Ohguma, K. Watanabe, N. Ootake, Silsesquioxane Derivatives and Process for Production Thereof, in: U.S. Patent (Ed.) United States, 2004.

[64] M.A. Hoque, Y. Kakihana, S. Shinke, Y. Kawakami, Polysiloxanes with Periodically Distributed Isomeric Double-Decker Silsesquioxane in the Main Chain, Macromolecules 42(9) (2009) 3309-3315.

[65] N. Liu, K. Wei, L. Wang, S.X. Zheng, Organic-inorganic polyimides with double decker silsesquioxane in the main chains, Polymer Chemistry 7(5) (2016) 1158-1167.

[66] K. Wei, L. Wang, S.X. Zheng, Organic-inorganic polyurethanes with 3,13-dihydroxypropyloctaphenyl double-decker silsesquioxane chain extender, Polymer Chemistry 4(5) (2013) 1491-1501.

ACKNOWLEDGMENTS

This thesis is a summary of my studies from 2020 to 2023 under the direction of Professor Joji Ohshita at Hiroshima University.

First and foremost, I would like to express my sincere appreciation to Professor Joji Ohshita, Graduate School of Advanced Science and Engineering, Hiroshima University, for his mentorship and helpful advice and encouragement.

I would like to express my deepest gratitude to Lecturer Takashi Hamada for supporting my research activities and providing guidance, advice, and wisdom, since the beginning.

I would like to thank Professor Atsushi Ikeda, Professor Masakoto Kanezashi, Professor Akinobu Naka, Professor Akira Uedono, Assistant Professor Yohei Adachi, Mr. Kenta Okada, Mr. Susumu Mineoi and Associate Professor Hiroyuki Koga for their useful advice and helps.

I am grateful to Mr. Katsuhiro Horata, Mr. Daiji Katsura, Mr. Tetsuya Maeda, Mr. Sun Weipeng, Ms. Wang Conghuan, Mr. Takashi Kai, Mr. Kohei Yamada, Mr. Keigo Kawakami, Mr. Kei Oshima, Ms. Maho Kurihara, Mr. Mitsuru Sakabe, Mr. Tetsuya Sugimoto, Mr. Arata Tanaka, Mr. Takumi Hasegawa, Mr. Tsubasa Yoshio, Mr. Lin Zhixin, Mr. Shota Terao, Mr. Ryuji Matsuura, Mr. Ryuto Miyazaki, and all other members of the past members of Element-Based Organic Materials Chemistry laboratory for their help and kindness.

Finally, I would like to express my appreciation to my mother Mutsumi Takase and my father Yasuhide Takase for their support and affection, without which it would have been very difficult to persevere through my many years of school.

Sakino Takase

January 2023